Politecnico di Milano

Facoltà di Ingegneria dei Sistemi

Corso di Laurea Magistrale in Ingegneria Biomedica

Analysis of T - Wave Alternans in ambulatory records using a new index: ADTWA.

Autore :
Simone Monacizzo
Matricola :
786649

Relatore :
prof. Luca Mainardi
Correlatori :
prof. Juan Pablo Martínez Cortés
prof. Roberto Sassi
ing. Valentina Corino

Scuola di Ingegneria Industriale e dell'Informazione
Corso di Laurea in Bioingegneria
Dipartimento di Elettronica, Informazione e Bioingegneria

Anno Accademico 2014/2015

ACKNOWLEDGMENTS

E' stato un viaggio lungo, tanto bello quanto tormentato e difficile! Tante persone mi sono state accanto in questi anni.

Voglio ringraziare prima di tutto il mio relatore, prof. Luca Mainardi, per la sua gentilezza ed il suo costante interesse nel mio lavoro.

Un grazie a Valentina, sempre estremamente disponibile e precisa nell'aiutarmi.

Gracias a Juan Pablo Martínez, por sus ideas y por su constante ayuda.

Y gracias a todos los investigadores del grupo I3A por las comidas, las cenas (italianas!), por el soporte mutuo, por las risas, por haber hecho mi estancia en Zaragoza inolvidable.

Grazie a tutte le persone che hanno condiviso un pezzo del percorso universitario assieme a me. Quel che da senso al viaggio è l'incontro, la condivisione. Poi in molti casi ci si perde di vista - normalissimo! Ma il confronto arricchisce sempre, lavorare con altri non significa solo crescere a livello professionale... significa, soprattutto, empatizzare, entrare in sintonia, crescere a livello umano.
Un grazie in particolare a Gennaro, Dzemila, Uros, Luca, per il supporto reciproco e le risate che ci han fatto prendere alla leggera quello che altrimenti sarebbe stato un semestre... bello pesante! Ed ancora, grazie ad Alice e Veronica, mie compagne di studio in diversi corsi della laurea magistrale.

Un ringraziamento ed un pensiero ai membri della mia squadra sportiva, 'La Michetta', perché siete stati per me come una seconda famiglia.

Ed infine, last but not least, il più grande grazie va alla mia famiglia, che mi è sempre stata vicina anche da lontano, senza di voi questo viaggio non l'avrei potuto neanche iniziare.

Simone

List of Figures

List of Tables

Contents

Abstract

Cardiovascular diseases are the major cause of death in adults and the elderly in the majority of the developed countries and in many developing countries. A great part of these deaths occur suddenly, shortly after the onset of the first symptoms, and are related to malignant ventricular arrhytmias that lead to a heart attack. This kind of outcome is known as *sudden cardiac death* (SCD) [40].

Implantable cardioverter defibrillators (ICD) are the most effective way of preventing SCD [5]. However, the implantation of an ICD is an invasive procedure with associated risks and a high cost. Therefore, it is necessary to determine *non-invasive risk markers* that identify patients at a higher risk of suffering malignant arrhytmias, so that invasive diagnostic test and treatments can be selectively applied only to those patients who will benefit the most, saving risk for the patients and also health-care costs.

Various non-invasive indices have been proposed to predict the risk of arrhytmias. Most of them are based either on the analysis of echocardiographic images [8] or on the analysis of electrocardiographic signals (QRS duration, QT dispersion, heart rate variability, etc.) [32]. The main limitation of existing indices is their low specificity and predictive value. One of the most promising non-invasive indices is T-wave alternans (TWA) [39]. Its prognostic value is being intensively studied and significant evidence of the relation between TWA and the susceptibility to ventricular fibrillation has been found in recent years [28]. This Master's Thesis work presents and assets a new method for evaluating the presence of TWA in ambulatory records (*Amplitude of Dominant T-Wave Alternans*).

Sommario

Le malattie cardiovascolari sono la causa principale di morte in adulti e anziani nella maggior parte dei Paesi sviluppati ed in molti dei Paesi in via di sviluppo. Una gran parte di queste morti avviene repentinamente, poco dopo la comparsa dei primi sintomi e risulta correlata ad aritmie ventricolari maligne che portano ad un attacco di cuore. Questo tipo di conseguenza viene chiamata morte cardiaca improvvisa (*Sudden Cardiac Death*, SCD) [40]. Il modo più efficace di prevenire la SCD è quello di usare defibrillatori cardioverter impiantabili (ICD) [5]. Tuttavia l'impianto di un ICD è una procedura invasiva, costosa e rischiosa. Per questo è necessario determinare *indicatori non invasivi di rischio* che siano in grado di identificare pazienti a più alto rischio di soffrire aritmie maligne, in modo che test invasivi diagnostici e trattamenti possano essere applicati selettivamente solo ai pazienti che ne trarrebbero i benefici maggiori, evitando rischi e spese sanitarie inutili.

Sono stati proposti diversi indici non invasivi in grado di predire il rischio di aritmie. La maggior parte di questi sono basati o sull'analisi di immagini ecocardiografiche [8] o sull'analisi di segnali elettrocardiografici (durata del QRS, dispersione del QT, variabilità del ritmo cardiaco ecc.) [32]. Il loro limite principale è la bassa specificità e valore predittivo. Uno dei più promettenti indici non invasivi è la alternanza dell'onda T (T-wave alternans, TWA) [39]. Negli ultimi anni c'è stato un intenso studio del suo valore prognostico e recentemente si è dimostrata una correlazione significativa tra TWA e suscettibilità a fibrillazione ventricolare [28].

La TWA è un'alterazione nella morfologia e nell'ampiezza dell'onda T che ha ordine di grandezza di qualche microvolt, per cui è invisibile all'occhio nudo e sono necessari metodi specifici di analisi del segnale ECG. Risulta inoltre fondamentale un'adeguata fase di pre-processing in quanto l'ampiezza del rumore elettrocardiografico dev'essere inferiore a quella della TWA.

Esistono due grosse categorie di metodi, i *monoderivazionali* ed i *multiderivazionali*. Della prima fanno parte tutti quelli che analizzano la TWA singolarmente per ogni derivazione. Il problema di questo tipo di analisi è che non tiene conto di certe caratteristiche di ridondanza spaziale e temporale tipiche della TWA. Tale problema è risolto dai metodi multiderivazionali che invece danno una informazione spaziale completa, basandosi su di algoritmi che ricavano l'informazione sull'alternanza da più derivazioni contemporaneamente.

Classicamente i metodi usati per misurare la TWA sono lo *Spectral Method* (SM) [14] ed il *Modified Moving Average Method* (MMAM) [27]. Si tratta di metodi monoderivazionali, la cui efficacia clinica è stata comprovata ed utilizzati in sistemi commerciali.
In ogni caso, in genere la TWA veniva misurata in particolari procedure cliniche come test da sforzo per frequenze cardiache comprese tra 100 e 125 bpm [33].
Nel 2010 è stato proposto un metodo [25], multiderivazionale, in grado di riconoscere la TWA in base alle sue caratteristiche di periodicità. L'obiettivo degli autori era arrivare a dimostrare che tale indice potesse misurare efficacemente la TWA in registrazioni elettrocardiografiche ed avesse un buon valore predittivo per la SCD. Per verificarlo, nel 2012 effetturono un secondo studio [24] in cui la TWA veniva misurata, con il loro metodo, su un database di registrazioni ECG Holter - quindi di durata vicina alle 24h, delle quali considerarono soltanto 650 provenienti da pazienti con ritmo sinusale. Quel che dimostrarono nel detto studio è che una TWA sostenuta *durante tutte le ore di registrazione* aveva effettivamente un buon valore prognostico per la morte cardiaca improvvisa.
Questo lavoro di tesi presenta un nuovo metodo per valutare la presenza di TWA in registrazioni cliniche (*ADTWA, Amplitude of Dominant T-Wave Alternans*), introdotto nel 2010 da Mainardi e Sassi [15]. Anche questo metodo è multiderivazionale e sfrutta il paradigma della onda T dominante (DTW), a sua volta basato su di un modello fisiologico di genesi dell'onda T ideato da van Oosterom nel 2001 [38]. La costruzione della DTW si basa su una Singular Value Decomposition (SVD), mentre l'ECG di superficie è approssimato da una combinazione lineare di più ripetizioni della stessa funzione, che ha la forma di un potenziale di transmembrana (TMP) di un miocita. L'efficacia metodologica dell'indice è stata già comprovata [36]. Rimaneva da valutare l'efficacia clinica, ossia il suo valore prognostico nel predire malattie cardiovascolari. Questo è l'obiettivo del presente lavoro di tesi.
Il lavoro è stato svolto dall'Aprile 2014 al Settembre 2014 presso la città di Zaragoza, all'interno del gruppo di ricercatori I3A, lo stesso in cui attualmente lavorano gli autori dello studio del 2012, sotto la supervisione del prof. Juan Pablo Martínez.
Utilizzando la stessa procedura dello studio precedente per quanto riguarda la parte di pre - processing e di selezione dei battiti, sono state ripetute le analisi sul database MUSIC [34] - utilizzando il nuovo indice - in modo tale da poter avere un confronto diretto ed immediato tra i risultati ottenuti nei due casi.
Alla fine dello studio, l'efficacia clinica del nuovo indice nel predire la SCD è stata comprovata. Le analisi statistiche hanno infatti prodotto un esito molto simile a quello dello studio precedente a dimostrazione del fatto che l'indice ADTWA può essere considerato un buon candidato per il riconoscimento e la misura della TWA in registrazioni elettrocardiografiche.

Extended abstract

Introduction

Cardiovascular diseases are the major cause of death in adults and the elderly in the majority of the developed countries and in many developing countries. A great part of these deaths occur suddenly, shortly after the onset of the first symptoms, and are related to malignant ventricular arrhytmias that lead to a heart attack. This kind of outcome is known as *sudden cardiac death* (SCD).

Implantable cardioverter defibrillators (ICD) are the most effective way of preventing SCD [5]. However, the implantation of an ICD is an invasive procedure with associated risks and a high cost. Therefore, it is necessary to determine *non-invasive risk markers* that identify patients at a higher risk of suffering malignant arrhytmias, so that invasive diagnostic test and treatments can be selectively applied only to those patients who will benefit the most, saving risk for the patients and also health-care costs.

Various non-invasive indices have been proposed to predict the risk of arrhytmias. Most of them are based either on the analysis of echocardiographic images [8] or on the analysis of electrocardiographic signals (QRS duration, QT dispersion, heart rate variability, etc.) [32]. The main limitation of existing indices is their low specificity and predictive value. One of the most promising non-invasive indices is **T-wave alternans (TWA)** [39]. Its prognostic value is being intensively studied and significant evidence of the relation between TWA and the susceptibility to ventricular fibrillation has been found in recent years [28].

TWA is an alteration in morphology and amplitude of T-wave which has got order of magnitude of some microvolts. It is invisible at a naked eye and may be difficult to discern by a computerized method due to intrinsic noise of electrocardiograms. That's why some specific methods of ECG signal processing are necessary, including an ad hoc preprocessing and sophisticated decision rules.

Different methods have been proposed in the past capable of measuring TWA. The first and still most used ones in clinical practice are *Spectral Method (SM)* [14] and *Modified Moving Average Method (MMAM)* [27]. They are single - lead methods, with proven clinical efficacy and commonly used in commercial systems.

They are classically used to measure TWA in some specific clinical procedures such as

stress tests and, in any case, analysis is restricted on heart rates comprised between 100 and 125 bpm [33].
In 2010 a new multilead index was developed [25] which detected TWA by maximizing the ECG signal at the TWA frequency that is 0.5 cycles per beat (cpb). In a second study [24] that method was used to measure TWA on a database of Holter ECG records (MUSIC : *MUerte Súbita en Insuficiencia Cardiaca* [34]) of which 650 with sinus rhythm were considered. A sustained TWA during all the hours of record was found to have a prognostic value for sudden cardiac death.
This Master's Thesis work presents and assets a new method to evaluate presence of TWA in ambulatory records (ADTWA, *Amplitude of Dominant T-Wave Alternans*), introduced in 2010 by Mainardi and Sassi [15]. This method is multilead and based on the paradigm of the Dominant T-Wave (DTW), which in turn is derived on a physiological model of T-wave genesis made by Van Oosterom in 2001 [38]. The construction of DTW is based on a Singular Value Decomposition (SVD), while the surface ECG is approximated by a linear combination of more repetitions of the same function, shaped as a trasmembrane potential (TMP) of a myocyte. The methodological efficacy of the index had already been proved [36]. Still, it was to verify its clinical efficacy, that is its prognostic value in predicting cardiovascular diseases.
This is the purpose of the present study.

Amplitude of Dominant T-Wave Alternans

A single measure of alternans can the be obtained across leads, l, by calculating the following index:

$$I = ADTWA = \max_{l} |\lambda_e u_e - \lambda_o u_o| \max_{t} |t_D| \tag{1}$$

Where:

- u_e and u_o are the first column of the matrix $\mathbf{U}$ obtained by singular value decomposition (SVD) of Ψ_e and Ψ_o which are the median templates for T-waves in even and odd beats respectively;
- λ_e and λ_o are the corrisponding eigenvalues;
- t_D is the Dominant T-Wave, which is estimated as the first column of the matrix $\mathbf{V}$ obtained by SVD of the vector $\Psi = (\Psi_e + \Psi_o)/2$.

Index (3.1) is labeled **Amplitude of Dominant T-wave Alternans (ADTWA)** to underline its relationship with the DTW paradigm. Given an Ecg recording, the steps needed for the computation of the parameters are the following:

- Detect the boundaries of a certain number of consecutive T waves. Then build the potential Ψ_e averaging all the T waves of an even number. The same should be done with odd T waves for Ψ_o. The averaging procedure improves the signal-to-noise ratio.
- Compute $v_1^T = t_D$ through SVD of matrix $\Psi = (\Psi_e + \Psi_o)/2$. Even and odd T waves are merged at this level of the analysis, as the physiological hypothesis is that the repolarization phase of the TMP does not vary in first approximation across following beats.
- Given t_D, estimate λ_e and u_e. The same should be done for Ψ_o, leading to λ_o and u_o.

Methods

650 patients with sinus rhythm were taken into account for analysis. Each record was pre - processed in order to eliminate baseline wander and high frequency noise with a pass band *Butterworth filter* of the third order, with cut off frequencies 0.5 Hz - 50 Hz. ECGs were analyzed in segments of 128 consecutive beats with 50% overlap between adjacent segments. Each segment was considered suitable for analysis if at least 80% of the beats composing it fulfilled the following conditions:

1. It is labeled as **normal sinus beat**;
2. Absolute value of each RR interval and the previous one is lower than 150 ms;
3. The difference between the **baseline** voltage measured at the PQ segment in that beat and the one measured in the previous one is lower than 300 μV.

After beat selection, each beat composing one single segment was aligned with respect to the QRS complex or with respect to the T-wave. Best results were achieved by using the first strategy probably for a precise physiological reason. Alternans, in fact, may disappear by doing the alignment on T-waves as it can be localized everywhere in the ST-T segment.
Indexes of alternans were calculated using three different methods.

- **AM Method** : Equation (3.1) is calculated on each segment kept for analysis and eventually the average is done for the values recorded during the 24 hours.
- **MM Method** : On each segment, a waveform of alternans is calculated, which is: $|\lambda_e u_e - \lambda_o u_o| * |t_D|$ - vector of lead factors multiplied for dominant T-Wave. Maximum of the averaged waveform is taken as an index of alternans.

- **VM Method** : After calculating a mean waveform, values recorded from the leads X,Y,Z are separated and magnitude of vectorcardiogram is calculated as following: $VCG = \sqrt{X^2 + Y^2 + Z^2}$. This way a waveform is obtained whose maximum is taken as an index of TWA.

Results

Indexes of alternans have been evaluated for all the segments composing the record and separating them into heart rate bins (60-70 bpm, 70-80 bpm, 80-90 bpm, 90-100 bpm, 100-110 bpm). Boxplots of those parameters have been plotted, in order to get a first graphical glimpse of the TWA dependence on heart rate. ROC curves have been calculated in order to get the best value which could discriminate subjects positive to our TWA test. Kaplan Meier survival curves were plotted after separating the whole population into two groups, ADTWA - positives and ADTWA - negatives. A subject was ADTWA - positive if his mean TWA activity was superior to a cut-off value, found by graphically inspecting ROC curves. Wilcoxon Log Rank test was performed in order to check the prognostic value of each index. Results got statistical significance for all the three methods ($p < 0.05$). The best ones were achieved by VM Method **($p = 0.003$)**, which was expected as it uses a measure that takes into account values from all the three orthogonal leads.

	Global	**60-70**	**70-80**	**80-90**	**90-100**	**100-110**
AM Method	7.19 [5.87 ÷ 8.82]	6.19 [4.62 ÷ 8.55]	7.86 [5.88 ÷ 10.45]	9.81 [7.25 ÷ 12.91]	11.66 [8.60 ÷ 15.70]	12.47 [9.12 ÷ 17.66]
MM Method	4.16 [3.23 ÷ 5.47]	3.75 [2.72 ÷ 5.43]	4.85 [3.57 ÷ 6.57]	6.01 [4.36 ÷ 8.19]	7.63 [5.22 ÷ 10.83]	8.12 [6.08 ÷ 13.12]
VM Method	4.85 [3.89 ÷ 6.17]	4.40 [3.21 ÷ 6.22]	5.82 [4.14 ÷ 7.62]	7.08 [5.18 ÷ 9.95]	8.80 [6.18 ÷ 13.05]	9.97 [7.01 ÷ 15.20]

TABLE 1: Median of ADTWA values and ranges (25th percentile ÷ 75th percentile). All values are expressed in microvolts. Heart rate bins are expressed in beats per minute (bpm).

	Chi - square	df	Sig
AM Method	4.955	1	0.027
MM Method	4.818	1	0.025
VM Method	8.487	1	0.003

TABLE 2: Global comparisons - Log Rank (Mantel Cox)

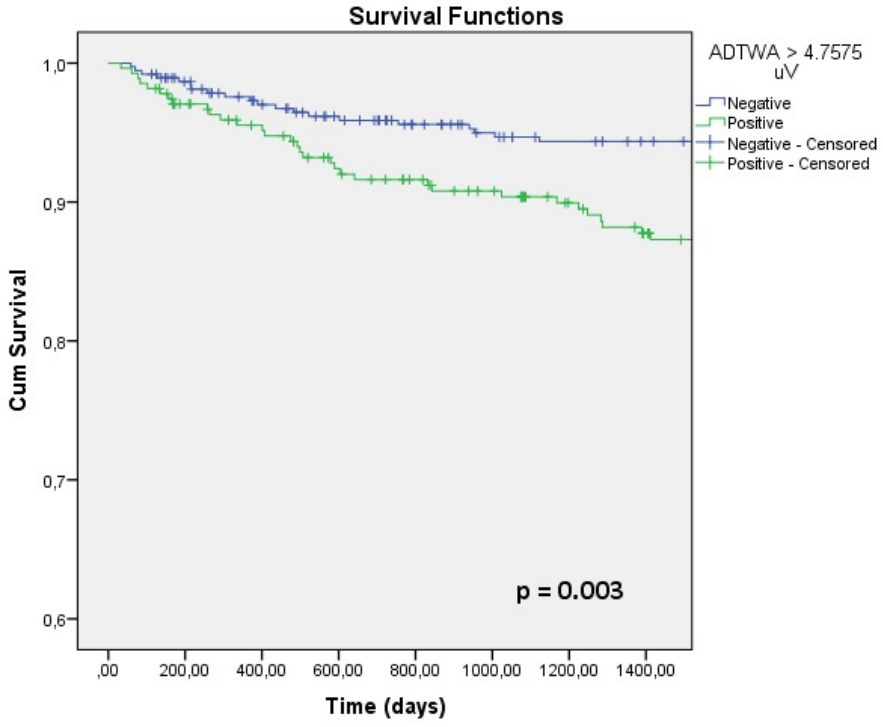

FIGURE 1: Kaplan Meier Survival Function for VM Method (ADTWA threshold = $4.7575\mu V$)

Discussion

Prognostic value of the new index for SCD was confirmed. Three indexes (ADTWA measured with AM Method, MM Method and VM Method) turned out to be good predictors of SCD in patients with CHF.

Thus ADTWA's methodological and clinical efficacy has been tested and these preliminary results suggest it can be used in clinical practice as a predictor of SCD.

Chapter 1

Introduction

1.1 Background

1.1.1 Electrocardiogram

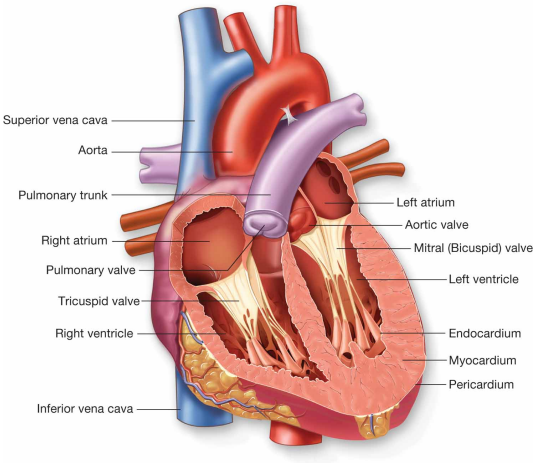

FIGURE 1.1: A human heart.

An **Electrocardiogram** (ECG) is a non-invasive electrical signal, acquired in the body surface, which describes the electrical activity of the heart [3] (fig 1.1).
The human heart is composed by two sides (left and right). Each one is made up of an *atrium* and a *ventricle* and the direction of blood flow is controlled by the presence of valves (the two atrioventricular and the two semilunar) which separate the atria from the ventricles or the ventricles from a blood vessel.
The heart is comprised of muscle (*myocardium*) that contracts rhythmically and drives the circulation of blood throughout the body. The whole cardiac activity is driven by the electro-mechanical coupling, that is, an electrical current spreads through the heart in a coordinated pattern which precedes the coordinated contraction of the myocardium

(*systole*). In practice, as a wave of electrical current spreads towars a myocardial fiber, a mechanical contraction is initiated. This phenomenon is called **excitation - contraction coupling**.

The fundamental electric property of human heart is **automaticity**: some cells exist which can spontaneously generate an electric pulse. The heart rhythm, in a healthy subject, is imposed by the *sinoatrial node (SA node)*, which is composed of a group of cells located at the intersection of the superior vena cava and the right atrium. Those kind of cells are known as **pacemaker cells**. They generate a normal sinus rhythm which is influenced by two systems, the *sympathetic* and the *parasympathetic*. Heart rate is fastened by the former, is slowed by the latter.

Thus a wave of depolarization is generated which spreads throughout the whole heart in a coordinated pattern. In fact, every cardiac cell has a negative potential across its membrane and the influx of positive ions (Ca^{2+} and Na^{+}) during the depolarization phase causes a rise of potential which, in turn, originates the mechanical contraction of the cardiac tissue. The first cells to depolarize are those of the *SA node*, thus generating a *wave of depolarization* which is transmitted to the atria and the ventricles through the *AV node*, located near the AV valve, which delays the passage of the impulse to the ventricles. This delay is functional, as atria have to pump all the blood to the ventricles before they start to contract. The current is then transmitted , through the *AV bundle*, to the *bundle of His*, which is divided into two branches - left and right - which conduct the impulse to the apex of the heart. Eventually the current is transmitted to the *Purkinje fibers* which lead the impulse upwards towards the ventricular myocardium. The return to rest potential is due to a net outflow of positive charge outside the membrane of the cardiac cells.

In summary, we distinguish four phases in one cardiac cycle (see fig 1.2):

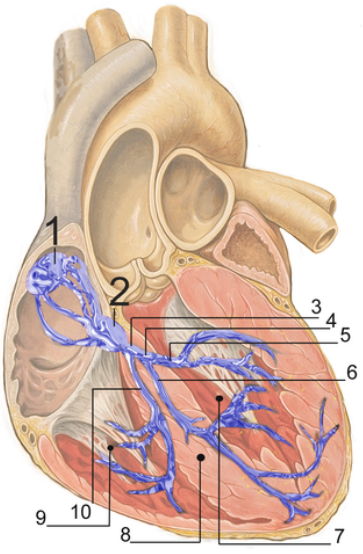

FIGURE 1.2: Heart. Conduction system 1-SA node. 2-AV node. 3. Bundle of His. 8. Septum

- The electrical stimulus originates from the SA node;
- The wave propagates through the atrium and reaches the AV node through the internodal pathways;
- The wave reaches the bundle of His;
- The wave reaches the ventricles through the bundle branches (left and right) and then through the Purkinje fibres.

Rest state (*repolarization*) is recovered through the outflow of net positive charge outside the cells membrane. This corresponds to a mechanical relaxation of the cardiac tissue (*diastole*).
The wave of electrical current which passes through the entire heart, triggering myocardial contraction, results in a measurable potential difference at the surface of the subject. This potential difference is recorded and amplified, originating the electrocardiographic signal (ECG).

1.1.2 Cellular Basis for ECG

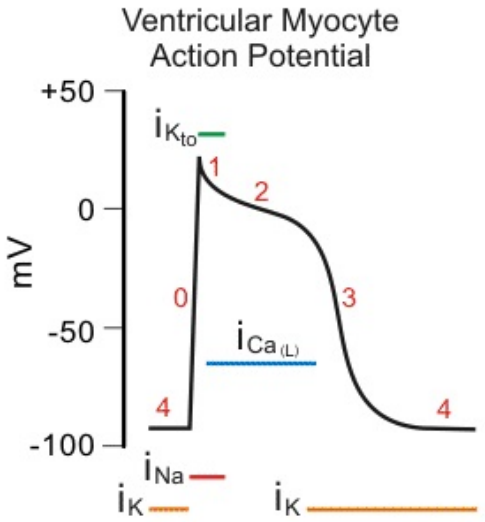

FIGURE 1.3: An action potential from a single ventricular myocyte.

Normally a difference in potential between interior and exterior of cardiac muscular cells (*myocytes*) is recorded, that is voltage inside the cell is more negative than outside. This is because of the distribution of the intra-cellular and extra-cellular electrolytes:

- Na^+
- K^+

- Ca^{++}
- $Cl-$

At rest, that is during that diastole, this difference in voltage, called *resting potential* is comprised between -50 and -60 mV for sinus node cells and between -80 and -90 mV for ventricular muscle cells and is maintained by the Na^+/K^+ pump, which extrudes 3 Na^+ ions for every 2 K^+ ions pumped in. Cardiac cells endowed with automaticity have the capability of *firing* (depolarizing) spontaneously when a critical *threshold potential* is reached. Potential which is approximately -40 mV for the cells of sinus node.
Rise and fall in potential are due to movements of electrolytes across the cell membrane through a number of channels, namely Sodium channels (INa), Potassium channels (IK) and Calcium channels (ICa). They permit or prevent the movement of ions depending upon transmembrane potential (TMP), modifying their conductance to a particular ion. Fig 1.3 represents a single *monophasic action potential* of a ventricular muscle cell, which describes changes in TMP plotted versus time. Sodium is the main electrolyte responsible for depolarization, whereas calcium is responsible for pacemaker cell depolarization. Three different phases can be distinguished:

- **Phase 1 - Depolarization**, which begins when a critical threshold is reached and sodium channels open. It manifests itself a positive spike in potential.
- **Phase 2 - Plateau**, the most distinctive feature of the cardiac action potential. During the plateau there is an approximate balance between inward-going calcium current and outward-going potassium current and the membrane conductance is relatively low. As a result, the transmembrane potential is kept constant.
- **Phase 3 - Repolarization**, the return to rest potential due to net outflow of K^+.

The duration of an action potential of a cardiac cell is called *Action Potential Duration* (ADP). Cells in different sites within the heart have different ADPs (see fig 1.4). In general, pacemaker cells have a *slow response*. They are characterized by a slower initial depolarization phase, a lower amplitude overshoot, a shorter and less stable plateau phase and repolarization to an unstable resting potential. Sinoatrial and atrioventricular nodal cells' action potentials are similarly shaped. Non - pacemaker atrial cells have action potentials shaped somewhere in the middle between the slow response nodal cells and the *fast response* cells (such as ventricular myocytes).

Eventually, this electrical conduction at a cellular scale results in a voltage difference recorded at the body surface (the ECG). The ECG is made up of different waves, each of which has a clear physiological meaning (fig 1.5):

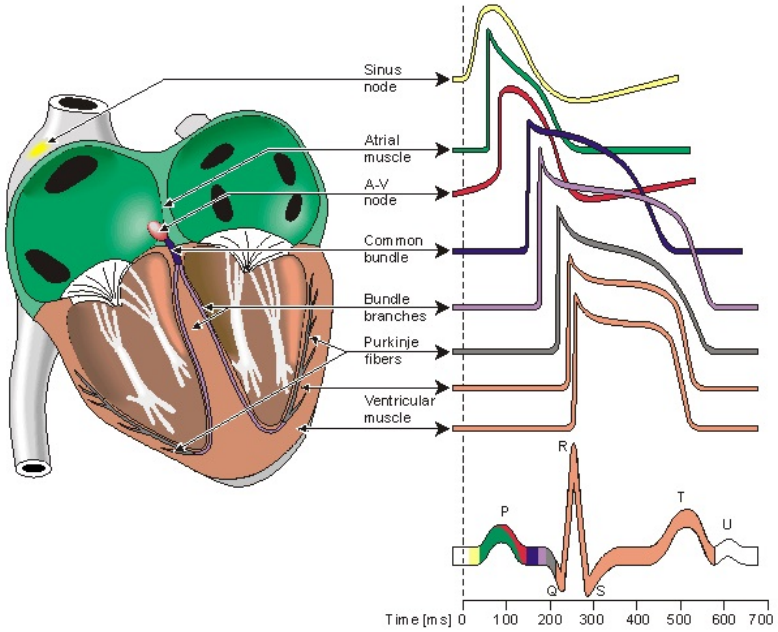

FIGURE 1.4: Representation of cardiac conduction system. To the right typical action potential waveforms recorded from myocytes in specific locations of the myocardium are displayed.

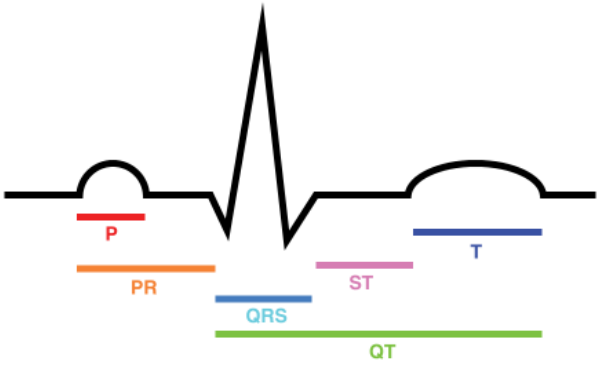

FIGURE 1.5: The ECG complex. P wave, PR interval, QRS complex, QT interval, ST segment, T wave

- When the depolarization stimulus propagates through the atria, a deflection can be seen on the ECG signal (**P-wave**). Atrial contraction (or *systole*) starts about 100 ms after the P-wave begins;
- The delay in the conduction when the stimulus passes through the A/V node is reflected as an isoelectric phase (**PR segment**);
- The spread of the electrical activity through the ventricular myocardium produces the **QRS complex**. Q wave corresponds to the depolarization of the interventricular septum, R wave is produced by the depolarization of the main mass of the ventricles and the S wave corresponds to the last phase of depolarization of the base of the ventricles.

- The **ST segment** represents the plateau in myocardial action potential, corresponding to the phase in which the ventricles contract and start to pump blood.
- Finally, the **T-wave** corresponds to the ventricular repolarization phase, which immediately precedes the ventricular relaxation.

One may wonder why atrial depolarization isn't represented in the ECG. The reason is it occurs at the same time of ventricular depolarization thus it's obscured by the much larger QRS complex.

1.1.3 Lead systems

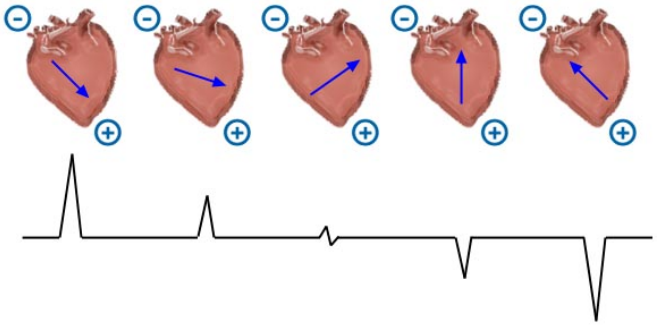

FIGURE 1.6: Projection of differently oriented cardiac vectors on the same lead

The voltage at the body surface is recorded through electrodes placed at the surface of the skin. The ensemble of the electrodes is referred to as the "lead system". Each lead represents a different view or projection of the electrical activity of the heart. A lead can be unipolar or bipolar. A *unipolar* lead is an electrode and the difference in potential is recorded between that electrode and a reference. A *bipolar* lead is made up of two electrodes and the voltage difference is recorded between those two electrodes. The placement of the electrodes defines the particular lead.
The lead system provides **spatial information**: in fact, it is the projection of the vector representing the cardiac activity on various angles (fig 1.6). The angle of the lead defines the particular angle of projection being used. Multiple lead systems could be used, varying from one simple couple of electrodes to the standard 12-leads system. Using one or another depends on what kind of clinical information are we looking for and on practical considerations.

The most widely used system is the 12-leads standard system, which is composed of:

- 3 *frontal* leads

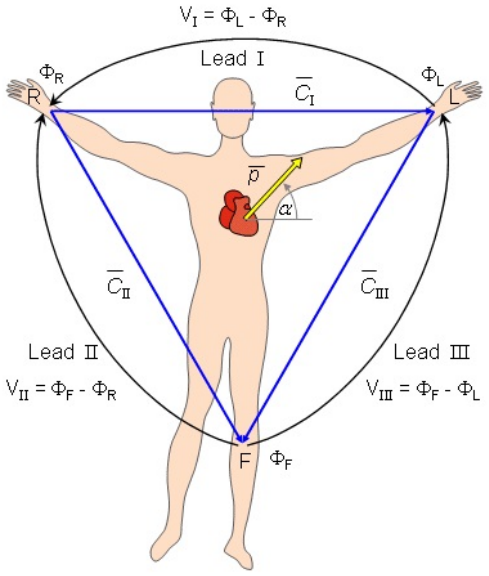

FIGURE 1.7: Einthoven limb leads and Einthoven triangle.

- 3 *augmented* leads
- 6 *precordial* leads

As far as the frontal leads is concerned (I, II, III), they are bipolar leads as they are made up of electrodes placed on the limbs - namely, two on each arm and one on the left - and the voltage difference is measured between these points (fig 1.7). The three points form the shape of a triangle named "*Einthoven's triangle*" with the heart at his center, which produces potential zero when the voltages are summed.
The three augmented leads are *unipolar leads*, in the sense that what is being measured is the voltage difference between one of the electrodes and a negative electrode which is the combination of the others, that is :

$$avR = RA - 1/2 * (LA + LL)$$

$$avL = LA - 1/2 * (RA + LL)$$

$$avF = LL - 1/2 * (RA + LA)$$

Finally, the precordial leads are placed directly on the chest : V1,V2,V3,V4,
V5,V6. They are considered to be unipolar leads as the voltage difference is taken between the positive electrode and a negative electrode that is *Wilson's central terminal*. Wilson's central terminal Vw is produced connecting the electrodes RA, LA and LL together, via a simple resistive network, to give an average potential across the body:

$$Vw = 1/3 * (RA + LA + LL)$$

Another often used lead system is the *orthogonal lead system*, which provides a kind of spatial information. In fact, the three leads **X**, **Y**, **Z**, represent the activity of the human heart in three orthogonal directions: they are the projection of the cardiac vector on the sagittal plane, the frontal plane, the transverse plane (1.8).

1.1.4 Vectorcardiography: description

The orthogonal lead system allows measurement and display of the electrical heart activity through the means of the **vectorcardiogram (VCG)**. In fact, it has been proved that, by enabling a better morphological interpretation of the electrical phenomena of the heart, vectorcardiography can help the diagnosis of different heart diseases [31].

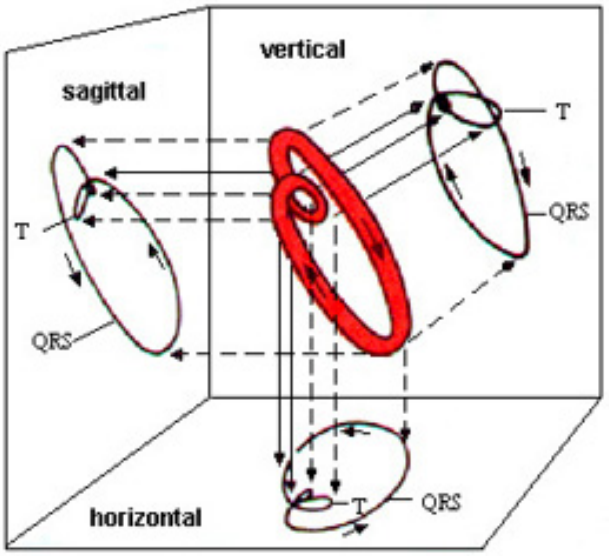

FIGURE 1.8: The principle of vectorcardiogram construction. The red curve depicts the loop made by the tip of the moving vector of the electric dipole of depolarization, in the cardiac muscle.

The principle the vectorcardiogram is based on is the fact that ventricular depolarization forms an instantaneous electric dipole. During the whole time of depolarization, many electric dipoles are formed which are represented as vectors. By mathematically summing all individual dipoles a global dipole of cardiac electrical activity is generated, which is represented by a **cardiac vector**. An example is shown in fig 1.9, which represents the cardiac vector during ventricular depolarization.
So, spatial vectorcardiography can be seen as a form of electrocardiography that tries to describe the electromotive force developed by the heart each instant as a single vector. Size and direction of the cardiac vector determine magnitude and direction of the electric field and the tip points towards the positive side. Therefore, vectocardiographic loops

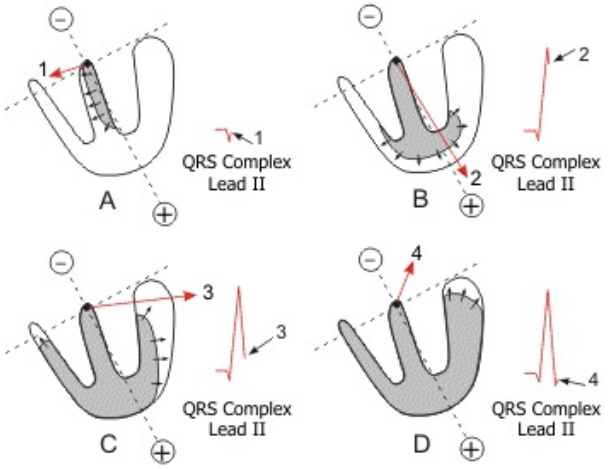

FIGURE 1.9: Cardiac vector during ventricular depolarization.

represent the position of all the instantaneous vectors, at each moment, during cardiac repolarization. Different loops can be obtained for the P, QRS, T and U waves (see fig. 1.10).
In vectorcardiography, due to the use of orthogonal leads, three spatial planes are determined : *vertical* or *frontal plane*, *horizontal plane* and *sagittal plane* (see fig 1.8).

1.1.5 Vectorcardiography: clinical advantages

VCG has a number of advantages for which it is preferable to a classic ECG record. Among them: [31]

- It provides **three-dimensional information of the electric activity of the atria and the ventricles** [37], showing in a clearer way than the ECG, the spatial orientation and the magnitude of the vectors at every moment.

- Has a greater sensitivity than the ECG in detecting **atrial enlargements** and greater sensitivity and specificity than the ECG in the diagnosis of **left ventricular enlargement** (LVE);

- Presents a greater correlation with the echocardiogram, when compared with the ECG, in determining the **left ventricular mass**;

- Presents a greater diagnostic sensitivity in comparison to the ECG in **acute myocardial infarction** (AMI);

- The evaluation of T-wave loop may be used as a 3D technique to assess **repolarization inhomogeneity** [9]. In fact changes in the morphology of the spatial T-wave loop were found to be associated to an enhanced scalar QT dispersion.

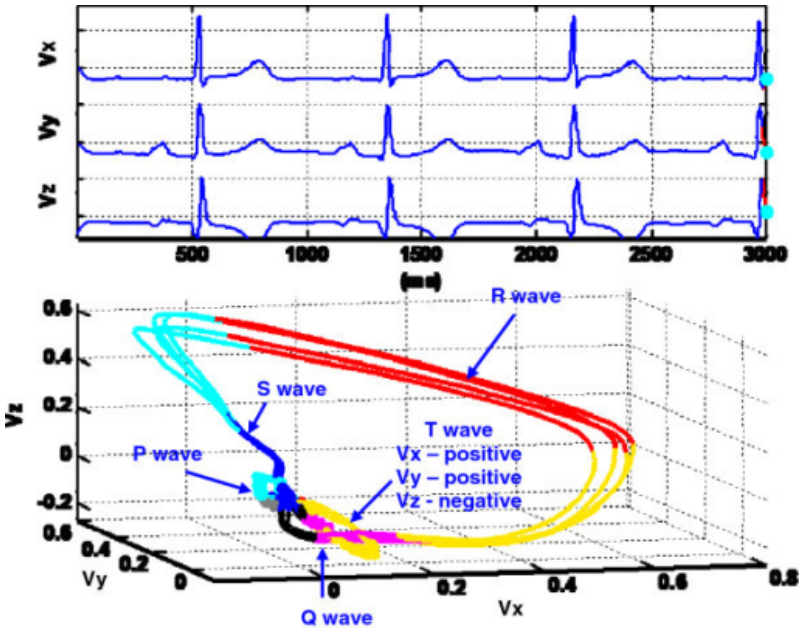

FIGURE 1.10: Examples of electrocardiographic loops.

In order to get the maximum information, a 15-lead approach should be used (12 standard + 3 orthogonal implemented in a 3D dimension).

With the use of computerized VCG, it is possible to determine where each loop begins and ends, establishing in a precise way, the ratio of length and width of T waves, and the estimation of the areas of the loops. In comparison with the traditional recording method, computerized VCG has a greater accuracy in measurement, besides a great processing velocity [11, 12].
In spite of the studies that show that the VCG and the ECG have a very similar diagnostic capacity [30], the VCG is still evolving and represents a low-cost method with great diagnostic value in different situations where electrocardiographic recording is doubtful.[6, 10]

1.1.6 ECG monitoring

ECG is a widely used tool in clinical practice. TWA is mainly being measured in three kinds of setups:

- ***Standard short ECG recording***

- ***Stress test***
  A stress test [7] is a kind of setup where the cardiovascular function of the patient

is being compared in two different conditions: at rest and during maximal, or sub-maximal, physical exertion. It usually involves walking on a treadmill or pedaling a stationary bike at increasing levels of difficulty, while electrocardiogram, heart rate and blood pressure are being monitored. The test ends when a maximal effort is reached or when abnormal heart rhythms are identified.

- ***MTWA test***
  MTWA tests [13] may be administered in a physician's office, hospital or outpatient clinic setting, in much the same way as a stress test. Electrodes are applied to the patient's torso and connected to wires that lead back to the MTWA system. Patients are then asked to walk on a treadmill for 5-10 minutes in order to gradually elevate the heart rate.
  Unlike stress testing, the heart rate is increased gradually and patients are not required to exercise until exhaustion. MTWA testing can also be conducted using pharmacologic agents or pacing to elevate the heart rate.

- ***Holter ECG***
  A Holter monitor [19] is a small, wearable device for continuously monitoring the electrical activity of the heart during a long period of time, of at least 24 hours. That's why Holter monitoring is much more likely to detect an abnormal heart rhythm when compared to the traditional ECG which lasts less than one minute. In this kind of the setup, the most widely used lead configuration is the 3-leads one due to patient's comfort reasons.

1.1.7 Ventricular fibrillation

When the electrical conduction system functions properly, the ECG presents a sinus rhythm, with a resting HR comprised between 50 and 100 bpm. An *arrhytmia* is any of a group of conditions in which the electrical activity of the heart is irregular or is faster or slower than normal [17]. In the worst case, a *ventricular fibrillation* [21] can be generated.
Ventricular fibrillation is the most serious cardiac disturbance. When it happens, the ventricles "fibrillate", that it they start to contract in a completely unsynchronized pattern. So heart's electrical activity becomes disordered and the ventricles start to quiver instead of effectively pumping blood. As an immediate consequence the person collapse within seconds. Fig 1.11 shows an example of ECG record when ventricular fibrillation occurs.

VF is treated by delivering a quick electric shock through the chest. It is done using a device called an external **defibrillator**. The electric shock can immediately restore the

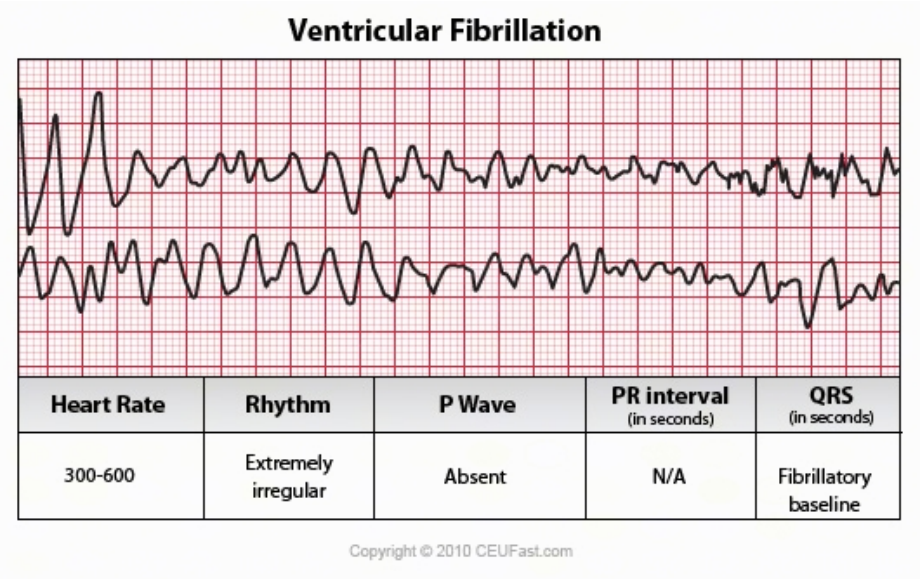

FIGURE 1.11: Example of ECG recording when ventricular fibrillation occurs.

heartbeat to a normal rhythm and should be done as quickly as possible.
Medicines may be given to control the heartbeat and heart function.
An **implantable cardioverter defibrillator (ICD)** [20] is a device that can be implanted in the chest wall of people who are at risk for this serious rhythm disorder. The ICD detects the dangerous heart rhythm and quickly sends a shock to correct it.
An ICD has wires with electrodes on the ends that connect to the patient's heart chambers. The ICD continuously monitors the heart rhythm and, when detects an abnormal or non-sinus rhythm, sends a low-energy electric pulse to restore the normal status.
If return to normal status isn't accomplished, a ventricular fibrillation may be occurring so the device sends an higher energy pulse. The high-energy pulses last for some milliseconds but can be painful.
A **pacemaker** [18] is another kind of device used to treat arrhythmias. It can send only low energy pulses so can treat less dangerous heart rhythm abnormalities, such as those occurring in the atria. Most recent ICDs can act both as pacemaker and defibrillators. Fig 1.12 explicates the difference between a pacemaker and a defibrillator.

1.1.8 Sudden Cardiac Death

Ventricular fibrillation is the most common cause of **Sudden Cardiac Death (SCD)** [40].
SCD is a different concept from **myocardial infarction** but it can occur during an heart attack. In fact myocardial infarction happens because a blockage in some arteries prevents the oxygen-rich blood to reach the heart. If heart cells don't receive enough oxygen they gradually suffer from mechanical damage, thus heart can't pump enough blood anymore.

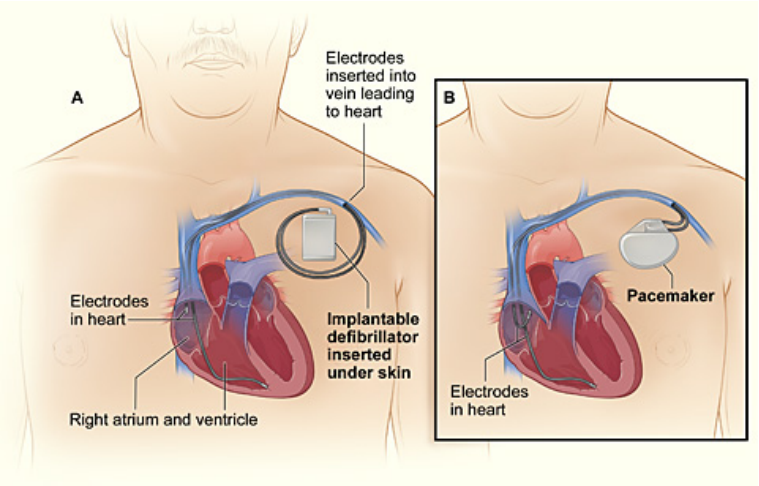

FIGURE 1.12: The image compares an ICD with a pacemaker. Figure A shows the location and general size of an ICD in the upper chest. The wires with electrodes on the ends are inserted into the heart through a vein in the upper chest. Figure B shows the location and general size of a pacemaker in the upper chest. The wires with electrodes on the ends are inserted into the heart through a vein in the upper chest.

SCD may be originated by a mechanical problem but the main cause is an *electric problem* of cardiac muscle cells. When a group of cells start to contract in a uncoordinated way, such as in ventricular fibrillation, ventricles may start to quiver. The consequence is that not enough blood will reach the brain.
Patients suffering SCD don't present the typical symptoms associated with heart attack, like chest pain and shortness of breath. Some people may experience some symptoms such as a racing heartbeat or feeling dizzy, alerting them that a potentially dangerous heart rhythm problem has started. In over half of the cases, however, sudden cardiac arrest occurs without prior symptoms: patients may be going with their typical daily business and suddenly collapse.
A number of causes are know to be associated with SCD, among them *coronary artery disease* and *heart failure*.

- *Coronary artery disease*
  When a stenosis of coronary arteries, namely the ones that take the blood flow to the heart muscles, occurs the consequence is a prolonged period of ischemia (lack of oxygen to the myocardium) which leads to a ventricular arrhytmia which, in turn, progresses into ventricular fibrillation, leading to the death of the subject.

- *Heart failure*
  Heart failure is a chronic, progressive condition in which the heart muscle is unable to pump enough blood through the heart to meet the body's needs for blood and oxygen. This is due to a weakness of the heart muscle, which thins the ventricle wall and, as a result, blood can't be effectively pumped out of the ventricle. A number of different causes can lead to heart failure. Examples include *coronary*

artery diseases, *heart attack*, *chronic high blood pressure*, *thyroid disease*, *kidney disease*, *diabetes*, *heart defects present at birth.*

1.1.9 T-wave genesis : ventricular repolarization

As previously said, T-wave genesis is linked to the ventricular repolarization phase. For a T wave to occur in a body surface ECG, there need to be some electromotive forces generated within the heart during the phase of ventricular repolarization. This is linked to the dispersion of ventricular repolarization along the myocardium. Two kind of dispersions actually exist:

- *Spatial variability*, as repolarization begins and ends in different times within the various portions of the ventricular tissue.
- *Temporal variability*, as duration of the phase 3 of the myocytes' transmembrane potential vary among different myocardial sites. It may also be defined as a difference in ADP (Action Potential Duration) between one beat and the next one. In order to distinguish between the two, the former may also be defined *"voltage dispersion"* of action potentials while the latter may also be called *"beat-to-beat dispersion"*. Excessive beat-to-beat dispersion is the phenomenon which leads to TWA (see following chapter).

Both types of gradient coexist: they may actually be additive, subtractive or neutral.

1.1.10 T-Wave Alternans

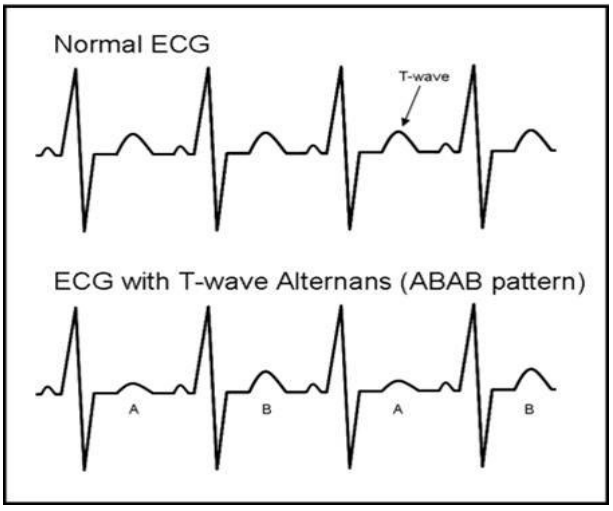

FIGURE 1.13: Normal ECG and ECG with T-wave Alternans

T-Wave Alternans is a repolarization abnormality manifesting itself as a periodic alteration of the T-wave morphology on the electrocardiogram with the period of two beats (see fig 1.13).

1.1.11 Physiological basis of TWA

As previously said, myocytes in the human heart do not repolarize at the same time, in fact a spatial dispersion of the repolarization times can be observed. Also, while depolarization happens on a faster time scale with a front moving along the myocardium, the current density during repolarization is dispersed across the ventricle. However, an increased repolarization heterogeneity paves the road to the development of fatal ventricular rhythm abnormalities. Above a critical heart rate threshold, repolarization of action potentials from adjacent regions of the ventricle alternate with opposite phase (discordant alternans), creating large spatial gradients in repolarization. Under these conditions, depolarizing wavefronts can become fractionated, allowing the development of unidirectional block, re-entry, and ventricular fibrillation.
T-wave alternans on the surface ECG is the epiphany of alternans in the repolarization patterns at the level of myocytes. In many cases the size of such alteration is small (about tens of microvolts) and buried into noise. Signal processing techniques are required in order to reveal microvolt TWA presence. Two models have been set forth to explain the presence of microvolt TWA [2, 22]. Basically both support the theory that changes in the dispersion of the repolarization times of the myocytes in turn modify the shape of the surface T-wave.
Fig 1.14 displays an example of ECG with TWA. Two beats are superimposed, then an alternans waveform is obtained as the difference between two median T-wave templates, one for odd beats and the other for even beats.

1.1.12 Objective and outline of the thesis

A new method has been proposed to measure T-wave alternans (Amplitude of Dominant T-Wave Alternans, ADTWA). Classically TWA was measured on a *single-lead* basis, that is information was taken analyzing each lead separately. However, TWA's characteristics of spatial and temporal redundancy only can be exploited if a joint measure from all the leads is done. Methods which work in this way are defined as *multilead*. Different multilead methods have been proposed in the past [25]. ADTWA is multilead and based on a physiological model which takes into account both *repolarization heterogeneity*

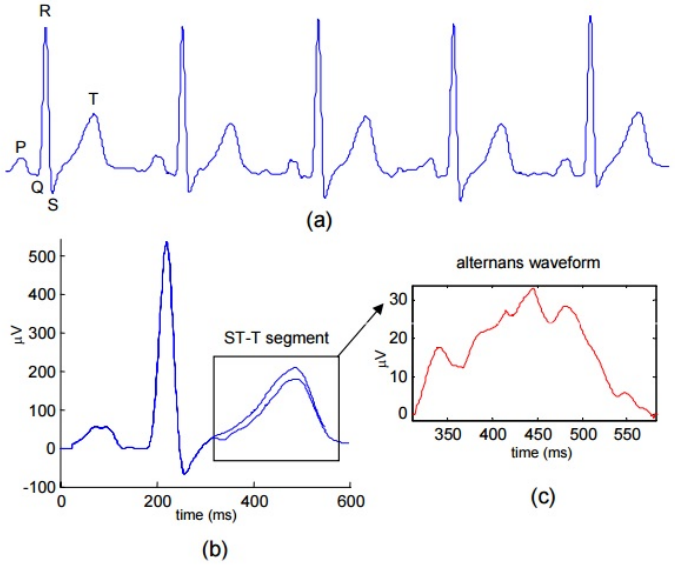

FIGURE 1.14: (a) Raw ECG signal. (b) Two consecutive beats are superimposed. (c) Alternans waverform (difference between odd and even beats).

across the myocardium as well as *random beat-to-beat variations in cells' activity* [38]. The reliability of ADTWA and its robustness against broadband noise have already been proved [36]. The objective of this Master's Thesis work is to apply the index to a real Holter ECG DB, in which the values of alternans had already been estimated with another multilead method [24], in order to check the clinical relevance of the new index in predicting SCD.
The following chapters of the thesis are organized in this way:

- **Chapter 2 : T-wave alternans assessment methods** State of art of TWA mesurement methods is presented. Spectral Method, Complex Demodulation Method and Modified Moving Average Method, which are the most widely used single-lead methods are described. A multilead method for analyzing TWA in ambulatory records, which was used in 2012 to detect alternans in the MUSIC database [24] is introduced. The last paragraph is dedicated to ADTWA: the physiological model it's based on, its mathematical algorithm and the methodological validation.

- **Chapter 3 : Methods** Methods used in ECG analysis are presented. The first paragraph is dedicated to the pre-processing steps - filtering, baseline wander removal and resampling. A self written algorithm to detect Q-onset points is described. The selection of beats is the same as the work of Monasterio et al., while beats alignment was done by checking the cross correlation with respect to the QRS complex or to the T-wave. Lastly, indexes of alternans are computed using three different methods - *AM Method*, *MM Method*, *VM Method* - and analyzed

for the whole population through *boxplots*, *Roc curves* and *Kaplan Meier survival functions*.

- **Chapter 4 : Materials** This chapter presents the Holter ECG database *(MUSIC)* used in the present study, describing the population under study and the study protocol.
- **Chapter 5 : Results** Results of the present study are shown. Boxplots of TWA indexes are represented in order to get a first graphical glimpse of the dependence of alternans on heart rate. ROC Curves and Kaplan Meier survival functions are plotted.
- **Chapter 6 : Discussion** A discussion on the results is done, focusing on their clinical relevance.

Chapter 2

T-wave alternans assestment methods

As we previously said, T-wave alternans is a beat-to-beat change which has the order of magnitude of microvolts, so it is very hard to see it at a naked eye and some methods of signal processing are required. In the last two decades, a variety of methods for automatic TWA analysis have been proposed. In 2005, Martinez and Olmos realized a complete summary and comparison between them [16]. In this chapter the most commonly used techniques are presented, focusing on the innovation introduced by the multi-lead methods in comparison with the single-lead ones.

2.1 Spectral method

Spectral Method was proposed in 1988 by Smith et al. [14]. A series of 128 consecutive heart beats is analyzed (fig 2.1, top). This number can change, but considering 128 beats represents a good compromise between reducing noise and tracking slow variation of alternans over time. The algorithm follows different steps:

- Time synchronized points from consecutive T-waves are extracted;
- *Cross correlation* of each beat with a template is done;
- A *time series* is built by measuring the voltage at the same points in time for all the 128 beats (fig 2.1, bottom left);

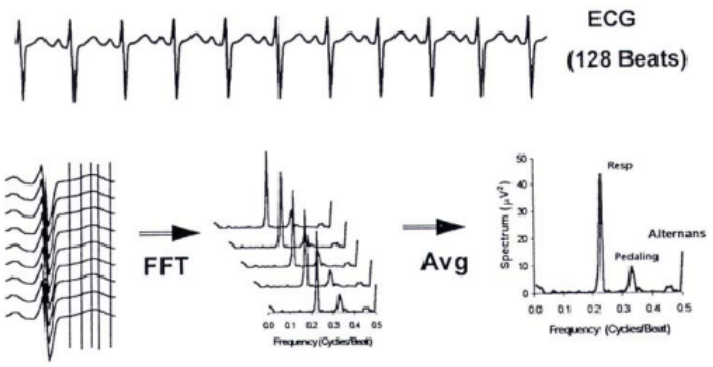

FIGURE 2.1: Spectral method explained

- Process is repeated multiple times, obtaining different spectra (fig 2.1, bottom center). The spectra are then averaged to form a composite *TWA spectrum*, whose frequencies are in the units of cycle per beat (cpb) (fig 2.1, bottom right);
- The value of the peak at 0.5cpb represents the TWA content in that time series.

An example of spectral analysis using Spectral Method is shown in fig 2.2. Spectral Method is included in some commercial equipment such as *CH2000*® and *Heartwave*®. It is the most widely used method to analyze exercise-induced TWA in stress tests [1].

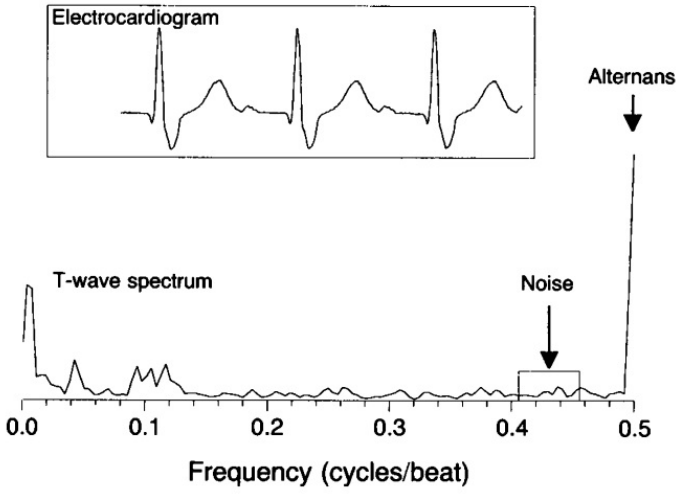

FIGURE 2.2: Example of spectral analysis of ECG, obtained from aligning 128 consecutive beats.

2.2 Complex demodulation method

In the **complex demodulation method** [4], the T-wave alternans is modeled as sinus wave whose frequency is f0=0.5 cpb, with variable amplitude and phase. Time series are obtained in the same way as in the spectral method and are then demodulated by multiplying them for the modeled TWA, so that the frequency components around f0 are shifted to low frequencies:

$$y[k,l] = x[k,l] * 2 * exp(j * 2 * pi * f0 * k)$$

Where x[k,l] is the l-th sample of the T-wave of the k-th beat. The low frequency alternans components are then extracted by using a low-pass filter. As the output of the filter, we have the beat-to-beat series of the alternans voltages for all the T-wave sample points.

2.3 Modified moving average method (MMAM)

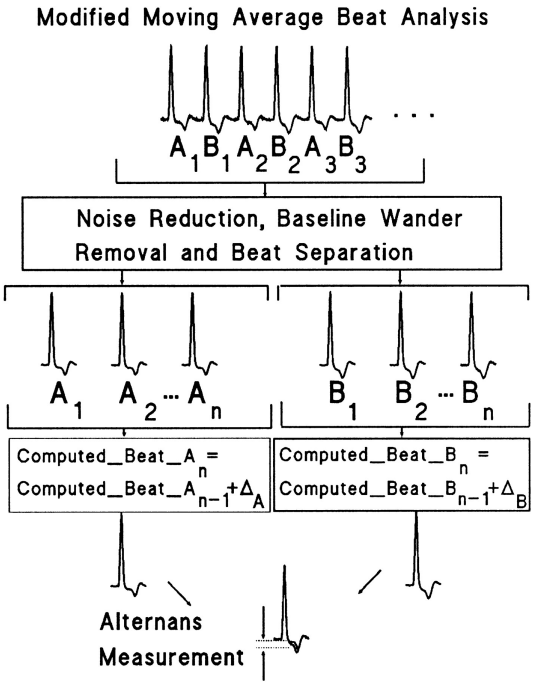

FIGURE 2.3: Modified moving average method explained

The **Modified Moving Average Method** [27] was set up to measure alternans in settings with *artifacts*, *noise* and *nonstationary data*. A recursive running average of

odd (A) and even (B) beats is continously computed. The alternans estimate for any ECG segment is then determined as the maximum difference between A and B within the ST segment and T-wave region. A flowchart of the algorithm can be seen in fig 2.3.

2.4 Laplacian Likelihood Ratio Method (LLR)

In 2005, a new robust method for estimating T-wave alternans was proposed by Juan Pablo Martínez and Salvador Olmos [16]. In their work, they showed that SM and CD methods can be understood as a **Generalized Likelihood Ratio Test (GLRT)** for TWA episodes in Gaussian noise. However the Gaussian noise model, usually assumed because of its mathematical simplicity and justified by the *central limit theorem*, does not characterize well some types of noise. In fact, in ECG recordings the presence of *artifacts*, *baseline wandering*, or *ectopic beats*, usually makes the noise in the beat-to-beat series to be more "spiky" than Gaussian noise. This method assumes a **Laplacian distribution**, which can model the noise in TWA series while keeping some mathematical tractability. Given a signal model including alternans and noise terms, the **maximum likelihood estimator (MLE)** and the **generalized likelihood ratio test (GLRT)** can be derived for TWA estimation and detection, respectively. So, the LLR computes the MLE and the GLRT for a Laplacian noise model to perform both estimation and detection of TWA.

2.5 A first multilead approach combining LLR and a linear transformation

All the methods previously described operate on a single-lead basis, that is they analyze each lead independently from the others. A first *multilead approach* (fig 2.4) was proposed by Monasterio and Martinez in 2008 [23].

The key idea of multilead analysis is to combine the information of the ECG leads to increase the *Alternans-Signal-to-Noise ratio* (ASNR) in the signal, that is, to improve the visibility of TWA over noise. A higher ASNR improves the detectability and estimation of TWA.
The preprocessing part is the same followed by all the single-lead methods and involves the basic steps of filtering, baseline wander removal, QRS detection and so on. Then a simple *detrending filter* is applied in order to eliminate the background ST-T complex.

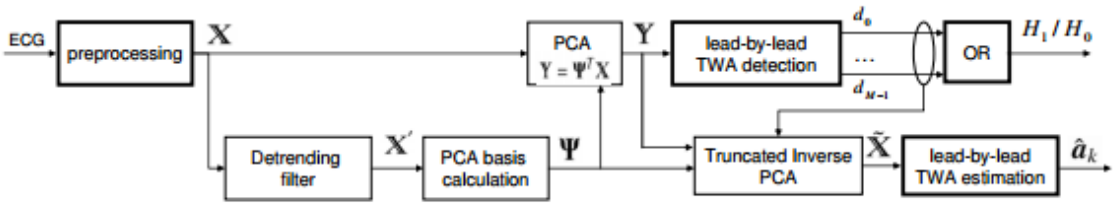

FIGURE 2.4: Block diagram of the multilead approach

So, the resulting matrix X' will be a mixture of TWA and noise, without the background ECG. A *trasformation matrix* Ψ is then applied. As the scheme is general, the matrix Ψ could be any transformation matrix able to enhance the TWA component (or separate it from the other components) in the transformed leads. In the case of Figure 2.4, PCA is applied to obtain the matrix Y, whose leads (rows of the matrix) will be denoted as *transformed leads*. The main idea is to project the alternans information of X in a subset of components, while most of the noise is projected into a different set of components. In this way, the TWA and the noise will appear separated and the TWA analysis will be easier.

TWA detection is then done exactly as the single lead method, in this case the LLRM and SM operate on the single leads. d_l is the result of the TWA detection on the single lead: if TWA is detected in lead l, then d_l=1, otherwise d_l=0. TWA detection is positive if d_l=1 for at least one lead (OR block).

The next step is that of the *signal reconstruction*, in order to be able to quantify the TWA amplitude in the original leads. Two new truncated matrices Ψ^T and Y^T are obtained keeping only the leads l of the original matrix for which d_l=1. A new signal is then reconstructed with the original matrices,

$$X_s = \Psi^T Y^T$$

where X_s is equivalent to a spatially filtered signal, where the filtering is aimed to preserve the alternans content. When no detection is obtained, X_s=0.

Finally, laplacian MLE is applied to the reconstructed data matrix in order to estimate the alternans waveform and amplitude. An example of alternans detection with this method is shown in fig. 2.5.

Two years later [25] this technique has been improved by using the method of the Periodic Component Analysis (πCA), descripted in the following paragraph.

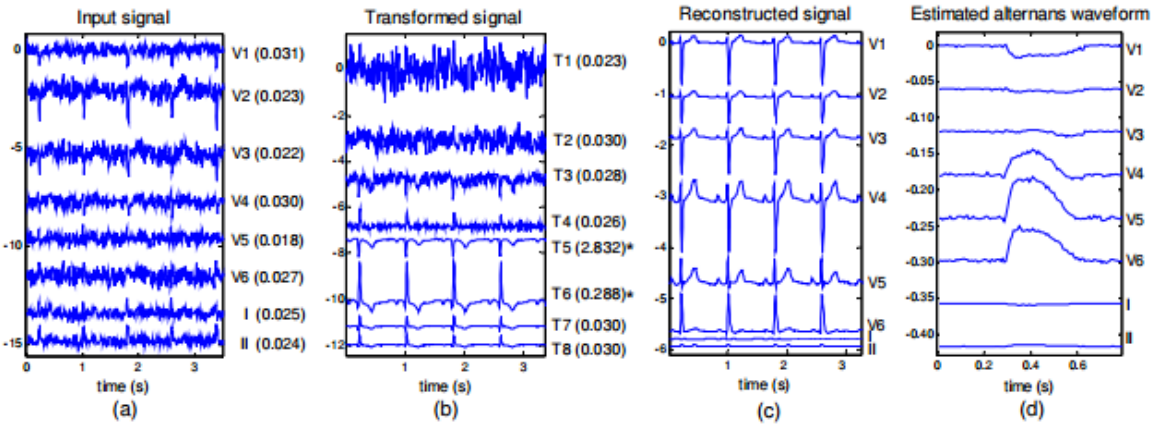

FIGURE 2.5: An example of multilead analysis.

2.5.1 Periodic Component Analysis (πCA)

Periodic Component Analysis (πCA) is an eigenvalue technique for analyzing periodic structure in multichannel signals. In this particular case, the aim is to find the transformation that maximizes the periodic structure of the signal at the TWA frequency, which is 0.5 cycles per beat (cpb), or equivalently at period m = 2 beats.
In practice, the projection $\tilde{y}' = w^T X'$ has to be found in order to maximize the signal at TWA frequency, with $\overline{w} = [w_1 w_2 ... w_L]^T$ is a column vector with L real weights.
In order to do so, a cost function has to be computed:

$$\epsilon(\overline{\boldsymbol{w}}, n) = \frac{||\tilde{\boldsymbol{y}}'^{(m)} - \tilde{\boldsymbol{y}}'||^2}{||\tilde{\boldsymbol{y}}'||^2} \tag{2.1}$$

Where $\tilde{y}'^{(m)} = w^T X'^{(m)}$ with m = 2 beats the period of TWA.
Expanding the right hand term of equation 2.1 in term of the weights **w** gives:

$$\epsilon(\mathbf{w}, n) = \frac{||\mathbf{w}^T \mathbf{X}'^{(m)} - \mathbf{w}^T \mathbf{X}'||^2}{||\mathbf{w}^T \mathbf{X}'||^2} =$$

$$\frac{||\mathbf{w}^T(\mathbf{X}'^{(m)} - \mathbf{X}'||^2)}{||\mathbf{w}^T \mathbf{X}'||^2} = \frac{\mathbf{w}^T(\mathbf{X}'^m - \mathbf{X}')(\mathbf{X}^{(m)} - \mathbf{X}')^T \mathbf{w}}{\mathbf{w}^T \mathbf{X}' \mathbf{X}'^T \mathbf{w}^T} = \frac{\mathbf{w}^T \hat{\mathbf{A}}_{X'}(m) \mathbf{w}}{\boldsymbol{w^T \hat{R}'_X w}}$$

In the resulting expression, both numerator and denominator are quadratic forms in the weights **w**. This ratio is known as the *Rayleigh quotient*. By the Rayleigh-Ritz theorem of linear algebra, the weights **w** that minimize the previous expression are given by the generalized eigenvector corresponding to the smallest generalized eigenvalue of the matrix pair $(\hat{A}_{X'}(m), \hat{R}_{X'})$.
Therefore, the transformation matrix Ψ is chosen as the generalized eigenvector matrix

of $(\hat{A}_{X'}(m), \hat{R}_{X'})$, with the eigenvectors (columns of Ψ) sorted according to the corresponding eigenvalues in ascending order of magnitude. In this way, the transformation

$$Y = \Psi^T X$$

projects the most periodic component into the first row of, that is, TWA — if present — is projected onto the first transformed lead and therefore the first column of Ψ can be interpreted as the spatial direction from which the periodic content of the signal is better observed.

2.6 Amplitude of Dominant T-Wave Alternans

Amplitude of Dominant T-Wave Alternans (ADTWA) [15] is a recently introduced index which offers a new perspective in the detection of T-wave alternans. As already pointed out, T-wave is the manifestation of the spatial dispersion of the ventricular repolarization, which is a natural property of the human heart. However, an amplified spatial repolarization could pave the road to the development of the mechanism of *reentry*, leading to ventricular arrhytmias and fibrillation. How to mathematically model well this mechanism, is still an open challenge (Malik, 2009). Neverthless, it is a fact that an increased T-wave alternans mirrors an increased dispersion in ventricular repolarization. The challenge is to find an index based on some physiological model which describes the repolarization phase through the means of some mathematical paradigm. In that sense, a metric of ECG repolarization heterogeneity has been presented by Sassi and Mainardi in 2011 (*V-index*) [35]. This metric was derived from the analysis of a biophysical model of the ECG [38], where repolarization is described by the Dominant T-Wave (DTW) paradigm. The model explains the shape of T-waves in each lead as a projection of a main waveform (the DTW) and its derivatives weighted by scalars, the lead factors. Through the means of a *singular value decomposition (SVD)* of the measured T-waves and using the definition of alternans a mathematical relation is then derived, in which each term has a clear physiological meaning.
Before describing the algorithm used, a presentation of the biophysical model on which the index is based is given in the next paragraphs.

2.6.1 A biophysical model of repolarization

Following the typical approach used in forward and inverse electrocardiography, myocytes are grouped together in "nodes", covering the entire myocardium. For each node, D(t) is a common transmembrane potential (TMP). While the steep upslope at

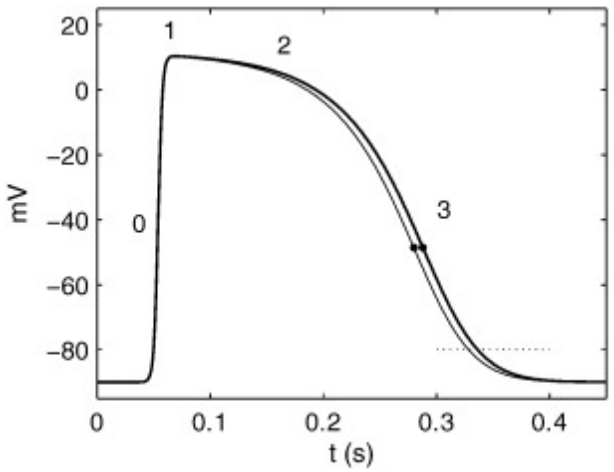

FIGURE 2.6: Sketch of cardiac action potentials for even (thin line) and odd (thick line) beats during alternans. Dots mark the repolarization times as the points of maximum downslope of the TMP.

depolarization is localized in time, the instant ρ_m in which the cells depolarize is not so clearly defined (see fig 2.6). Here, as in Van Oosterom's work [38], the point of maximum downslope of the TMP was selected. Doing so the average repolarization time across all the nodes in the ventricles $\overline{\rho}(k) = \sum_{m=1}^{M} \rho_m(k)/M$, for the beat k, is related to the position of the peak of the T-wave. Then the repolarization time of the m^{th} "node" is taken to be

$$\rho_m(k) = \overline{\rho}(k) + \Delta\rho_m(k) \tag{2.2}$$

where $\Delta\rho_m(k) = \overline{\rho}(k) + \Delta\rho_m(k) \ll \overline{\rho}(k)$ is the dispersion ("heterogeneity") with respect to $\overline{\rho}(k)$ and by definition, $\sum_{m=1}^{M} \Delta\rho_m(k) = 0$.

2.6.2 A first order approximation for the T-wave: the dominant T-wave paradigm

Consequently a mathematical relationship between the repolarization phase of TMP, their dispersions, and observable T-waves morphologies has been formalized. The potentials recorded at the skin during ventricular repolarization are represented by ψ, an [L x N] matrix containing the N ECG samples recorded from L leads. Assuming linearity of the conductive medium [29], these potentials can be related to the repolarization phase of transmembrane action potential (TMP), D(t), by the following equation:

$$\Psi = \mathbf{A} \cdot \begin{bmatrix} D(t-\rho_1) \\ D(t-\rho_2) \\ \dots \\ D(t-\rho_M) \end{bmatrix} \tag{2.3}$$

where **A** is an [L x N] transfer matrix that accounts for both the volume conductor properties (geometry and conductivity) and the solid angle under which the single source contributes to the potential ψ in each lead.
In eq. 2.3 D(t) is supposed to be identical across cells, but shifted by a factor ρ_i, which identifies the specific repolarization time of each cell. Writing ρ_i in terms of its distance from the mean repolarization time $\overline{\rho_i}$ (ie, $\rho_i = \overline{\rho} + \Delta\rho_i$) and assuming $\Delta\rho_i \ll \overline{\rho}$, the function D(t) can be expanded in series around $\overline{\rho}$ leading to the following model:

$$\Psi = -\mathbf{A} \cdot \begin{bmatrix} \Delta\rho_1 \\ \Delta\rho_2 \\ \dots \\ \Delta\rho_M \end{bmatrix} \cdot \left. \frac{dD(\tau)}{d\tau} \right|_{\tau=t-\overline{\rho}} + o(\Delta^2\rho_m) \tag{2.4}$$

In most cases, the linear term in eq. 2.4 dominates and when this happens, we have

$$\Psi = -\mathbf{A}\dot{\Delta}\rho \cdot \left. \frac{dD(\tau)}{d\tau} \right|_{\tau=t-\overline{\rho}} = wT_D, \tag{2.5}$$

Where $\Delta\rho$ is composed of the different delays $\Delta\rho_i$. The first derivative of the repolarization curve $T_D = \frac{dD(\tau)}{d\tau}$ becomes the dominant contribute to T waves and was therefore named *dominant T-wave* (DTW). It is worth noticing that when the approximation 2.5 holds, the T waves measured on the thorax are only a rescaled version of T_D, being $w = A\Delta\rho$ a vector of lead factors determining amplitude and signs of the T waves. Interestingly, this form shows that measured T wave on the skin depends on both the repolarization curve of TMP and the dispersion of repolarization times, two entities that are affected by alternans at cellular levels.

2.6.3 Physiological model

Studies performed at cellular level demonstrated the existence of alternans in TMP of myocites. Interestingly, looking at the downslope during phase 3 of the TMP, it appears that the steepness of the recovery phase does not change between even and odd beats, especially for moderate or moderately high heart rate (see fig. 2.6). This means that, in first approximation, the DTW is not affected during alternans, and thus, we will keep it as a constant in our analysis.
Ψ_e and Ψ_o are the surface T waves for even and odd beats, respectively. Under the previous assumption, their first order (rank 1) approximations are given by $\Psi_e \approx w_e \cdot T_D$

and $\Psi_o \approx w_o \cdot T_D$ where the DTW T_D is, as stated before, taken to be constant across beats. Following its definition, TWA can be quantified by considering the maximum absolute differences in the T waves of even and odd beats

$$TWA = \max_t |\Psi_e - \Psi_o| \approx |\Psi_e - \Psi_o| \max_t |T_D| = |A(\Delta\rho_e - \Delta\rho_o)| \max_t |T_D| \tag{2.6}$$

The remarkable aspect of Eq. 2.6 is that information on TWA is summarized into 2 factors:

- The $\max_t |T_D|$ term, which is related to the *repolarization phase of the TMPs*,
- The difference $|A(\Delta\rho_e - \Delta\rho_o)|$, which accounts for *differences* in the *repolarization times* among *even and odd beats*

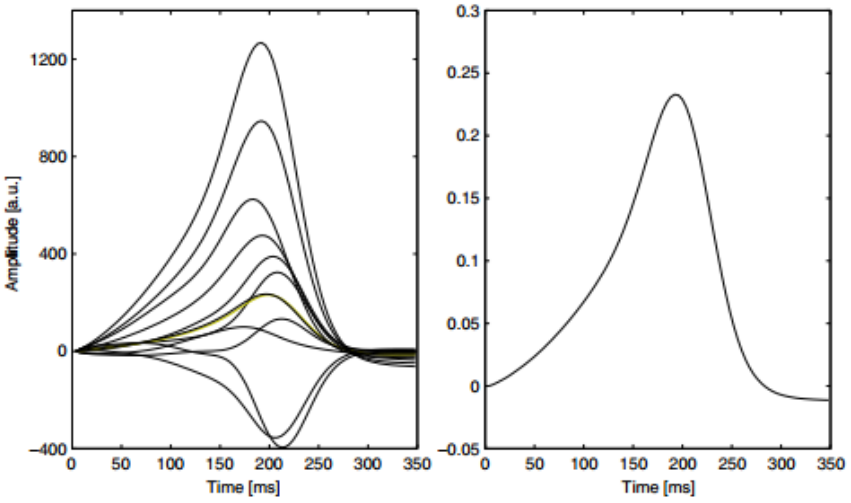

FIGURE 2.7: Dominant T-Wave estimation. To the left some examples of DTWs are shown. To the right, one single DTW is represented which has been rescaled to unit norm.

Thus, relation 2.6 provides a direct link between TWA and factors that are supposed to have originated it. To compute it, we need a first method to estimate T_D and a second one to obtain the weights w_e and w_o once given T_D.
An estimated of the DTW can be obtained through the minimization of the Frobenius norm of the error

$$\epsilon = \|\Psi - wT_D\|_F \tag{2.7}$$

between the measured T waves, Ψ, and their approximations by the first-order term of Eq. 2.5. In Eq. 2.7 T_D is unknown and estimated as v_1^T which is the first column of

the matrix V derived from a SVD of Ψ, rescaled to unit norm. An example of DTWs estimated with this method can be seen in fig. 2.7.

An index of TWA
Eq. 2.6 expresses the amount of TWA on each lead separately. A single index of alternans can the be obtained across leads, l, as

$$I = \max_l |A(\Delta\rho_e - \Delta\rho_o)| \max_t |T_D| \tag{2.8}$$

where the first maximum is taken across the rows of the vector $|A(\Delta\rho_e - \Delta\rho_o)|$. The index can be rewritten as:

$$I = ADTWA = \max_l |\lambda_e u_e - \lambda_o u_o| \max_t |t_D| \tag{2.9}$$

and will be labeled **Amplitude of Dominant T-wave Alternans (ADTWA)** to underline its relationship with the DTW paradigm. Given an Ecg recording, the steps needed for its computation are the following:

- Detect the boundaries of a certain number of consecutive T waves. Then build the potential Ψ_e averaging all the T waves of an even number. The same should be done with odd T waves for Ψ_o. The averaging procedure improves the signal-to-noise ratio, but as an alternative, a beat-to-beat analysis could be performed considering a single even and odd beat at a time.
- Compute $v_1^T = t_D$ through SVD of matrix $\Psi = (\Psi_e + \Psi_o)/2$. Even and odd T waves are merged at this level of the analysis, as our physiological hypothesis is that the repolarization phase of the TMP does not vary in first approximation across following beats.
- Given t_D, estimate λ_e and u_e. The same should be done for Ψ_o, leading to λ_o and u_o.
- Evaluate the ADTWA by eq. 2.9.

2.6.4 ADTWA validation

Two kinds of validation have to be done in order to prove an index's efficacy: methodological evaluation and clinical evaluation.
Methodological evaluation consists in quantification of the method's detection power and estimation accuracy. **Clinical evaluation** assets the utility of TWA measurements

as cardiac risk markers. It is preferable to do a methodological evaluation before going on with the clinical analysis.

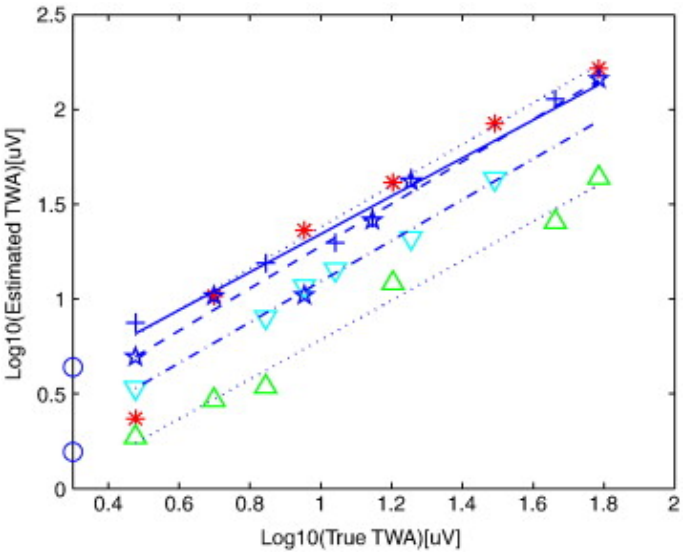

FIGURE 2.8: Comparison of estimated vs true TWA amplitudes.

A first methodological evaluation of the method was done by Mainardi and Sassi [15], who analyzed data coming from the Physionet/Computers in Cardiology (CinC) Challenge 2008, which contains 100 multichannel ECG records (2,3 or 12 leads) sampled at 500 Hz, with 16 bit resolution over a $\pm 32mV$ range. Thirty-two of these records were synthetic and created using 5 different models in which the TWA was added at different extents (range, $2 - 60\mu V$). The artificial TWA was created by modulating the T-wave loop of a synthetic vectorcardiogram, then projecting the vectorcardiogram onto 12 scalar ECG leads using 5 individual Dower transform matrices [26]. Six levels of TWA were added to each ECG model, for a total of 30 simulated ECG.
Results of validation are showed in fig 2.8, which displays the comparison between the estimated TWA amplitude, using the newly introduced index ADTWA and the ones used to build the synthetic records ("real"). Only the 32 synthetic records were used for validation. A good linear relationship has been found between estimated and expected TWA values ($R^2 = 0.9898 \pm 0.0100$) ($mean \pm SD$).
It is interesting that regression lines have different slopes for different ECG models. This is well expected from the way the synthetic ECG were generated. In fact, they were obtained by applying different Dower matrices, which implies different transfer matrices **A** for each ECG model and, thus, a different sensitivity of the index.

2.6.5 Why ADTWA?

A number of strengths makes ADTWA promising:

- The **DTW** directly derives from a *physiological model* and reflects the *repolarization stage* of the *myocytes transmembrane potential*;
- ADTWA uses **Singular Value Decomposition** (SVD) to compute the DTW thus it benefits from SVD's *resilience towards uncorrelated noises*;
- In considering **multiple leads** it implicitly overcomes one of TWA measurement's typical problems, that *TWA magnitude may be lead-dependent.*

Given the high coefficient of correlation between prediction and true values of TWA, for each model considered, performance obtained were encouraging on simulated ECGs, slightly better than those achieved by Spetral Method (SM)[15].
So we believed ADTWA could be a good candidate for the development of a new TWA detection algorithm. But first, we needed to test the performance of the method on real, ambulatory records in order to clinically validate the method.
This is the objective of the present study.

Chapter 3

Methods

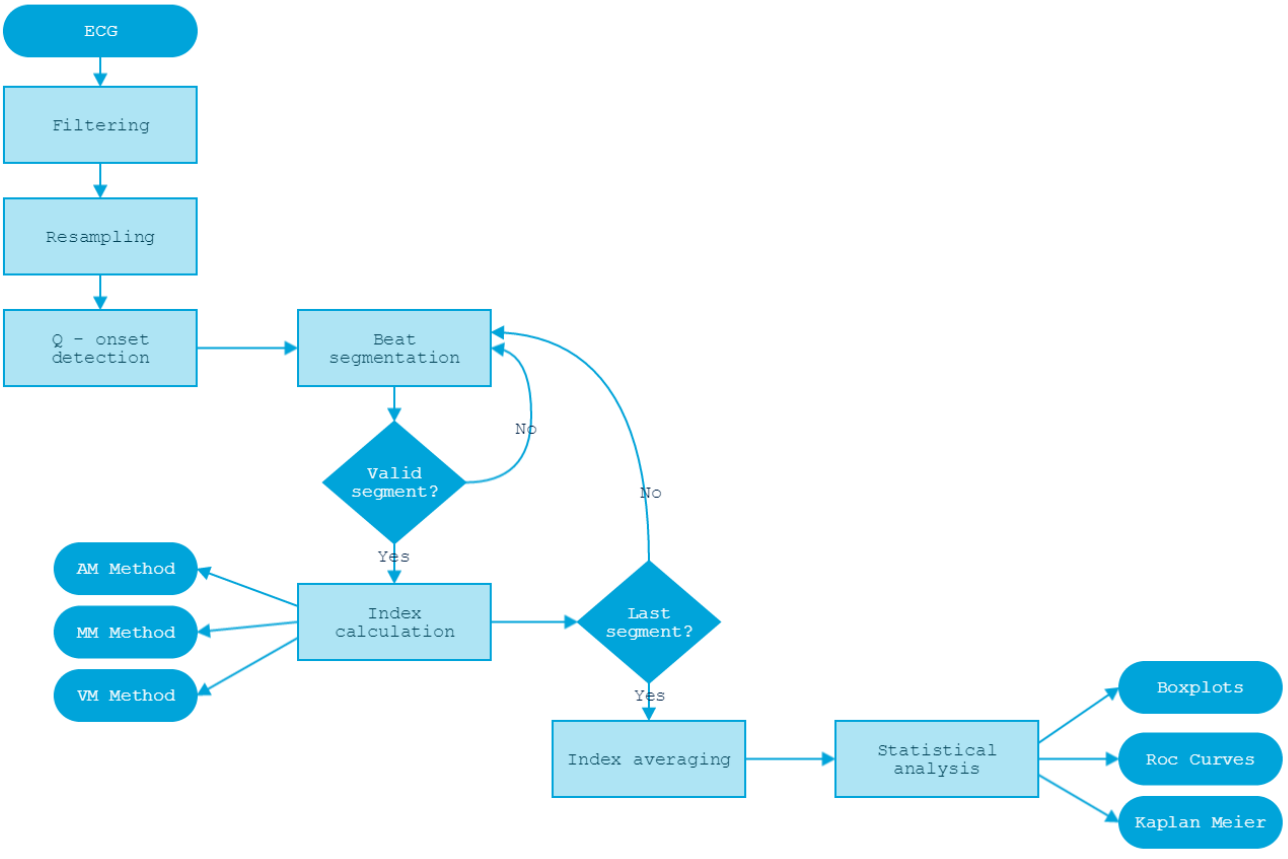

FIGURE 3.1: Flowchart of the methods used.

A flowchart of the methods we used is shown in figure 3.1. Every ECG is *filtered* in order to remove baseline wander and high frequency noise, then *resampled* - from 200 Hz to 1000 Hz, and finally *Q-onset points* are detected. *Beat segmentation* is done, i.e., the ECG recording is divided into segments and for each valid one, indexes of TWA

are calculated. Eventually, when the last segment is processed, *statistical analysis* is performed. Every step will be described in details in the following paragraphs.

3.1 Pre-processing

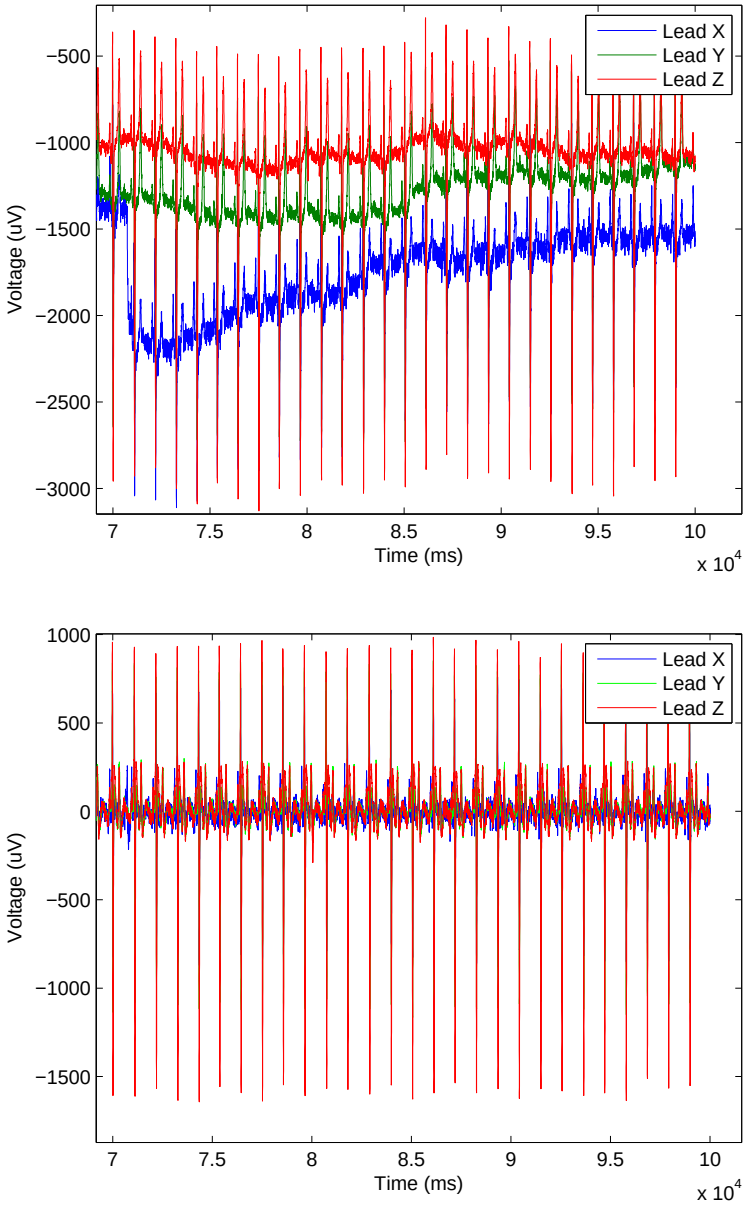

FIGURE 3.2: An excerpt of ECG before and after baseline wander removal is shown. Signal coming from the three leads X,Y,Z is represented in both cases.

Generally speaking, the aim of pre-processing steps is to improve the *signal to noise ratio* of the ECG for more accurate analysis and measurement. Accurate TWA measurement in ambulatory recordings is technically challenging due to the confounding effects of time-varying periodic and non periodic noise such as movement, myopotentials or respiration

and data nonstationarity from changing heart rate, TWA magnitude, or ectopic beats. Here the main categories of noise are summarized :

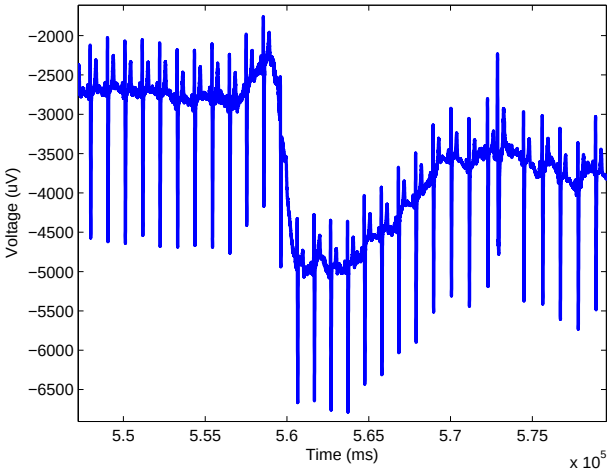

FIGURE 3.3: Example of noisy ECG with baseline wander.

- **Low frequency *baseline wander* (BW)**. It's a low frequency noise (0.5 - 1 Hz) which interferes with the standard ECG activity, in such a way that an isoelectric line can't be correctly defined (see fig 3.3). It may manifests as an high amplitude noise when analyzing the beat-to-beat series, masking subtle TWA or generating false detections. Therefore, it has to be corrected before proceeding with further analysis.
- High frequency random noises caused by ***power line interference*** (50 or 60Hz).

We used a Butterworth band pass filter (3rd order, cut off frequencies 0.5 Hz - 50 Hz). *Zero-phase filter* has been applied in order not to introduce phase distortion. As a result, baseline wander as well as high frequency noise are removed while keeping the information on TWA.
Figg. 3.2 shows an excerpt of ECG before and after band pass filtering.

3.1.1 Resampling

Every ECG has been resampled from 200 Hz to 1000 Hz in order to keep the duration of one sample equal to one millisecond.

3.2 Fiducial point detection

The QRS complexes were already detected by a detector (Aristotle), so the positions of the R-peaks for every beat were available. Positions of R peaks have been used to

calculate the RR intervals and thus the heart rate for each beat. A simple algorithm was written in order to calculate the Q-onset of every beat:

- First derivative of the signal is calculated (Butterworth high pass filter, third order);
- A threshold is set (15 μV, found by graphically inspecting the first derivative of the ECG);
- If the derivative is below threshold in one point and (at least) in the following three ones, that point is the Q onset.

Detection of Q onset was necessary as PQ interval was chosen as isolectric line after baseline wander removal. An example of detection is shown in fig 3.4.

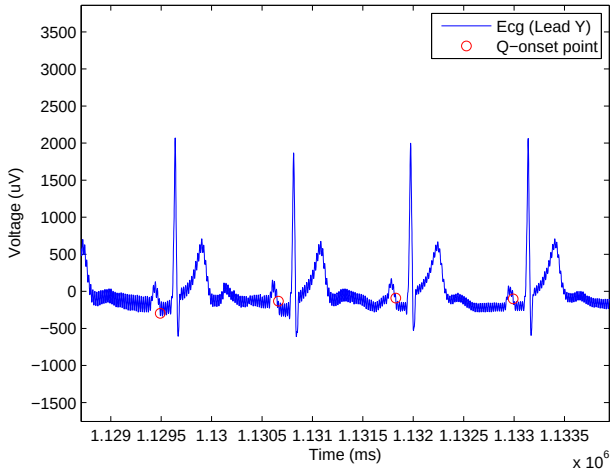

FIGURE 3.4: Example of Q onset detection. In blue signal coming from Lead Y is represented. Red dots are Q-onset points as recognized by the algorithm.

3.3 Beat selection

Not every beat could be taken into account for analysis. We excluded *ectopic* beats from the analysis, as they mirror non-physiological dynamics. ECGs were analyzed in segments of 128 beats with a 50% overlap between adjacent segments. Each segment was included in automatic TWA analysis if:

- (1) the difference between the maximum and the minimum instantaneous heart rate (HR) during the segment was inferior to **20 beats/min**
- (2) at least 80% of the beats fulfilled the following conditions:
  - (a) it was labeled as **normal sinus beat**

- (b) the difference between each RR interval and the previous one was lower than **150 ms**,
- (c) the difference between the **baseline** voltage measured at the PQ segment in that beat and the one measured in the preceding beat was inferior to 300 microvolts.

The rules are the same followed by Monasterio et al. [24]. While in their work the segments were always 128-beats long, we decided to exclude from analysis beats that didn't respect the conditions previously described. That's why our segments were generally shorter than 128 beats.

3.4 Beat alignment

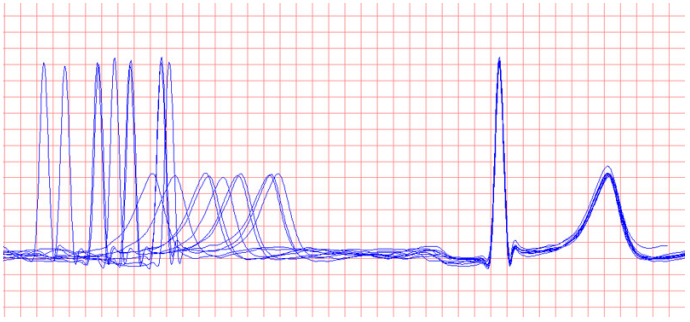

FIGURE 3.5: Example of beat alignment.

Next step was aligning all the beats with respect to a common point (see fig 3.5). This was necessary in order to get a common frame of reference in time. Two different strategies were followed. First one was to align on QRS complexes, second one to align on T-waves.

3.4.1 Alignment on QRS complex

The first strategy was to align on QRS complex. Positions of R peaks were available. Alignment was done by calculating a mean QRS complex template, computing the cross correlation matrix of each beat with the template and eventually calculating the delay between each QRS complex and the mean QRS complex. This way alternans is kept intact, as T-waves are not touched during the procedure.

3.4.2 Alignment on T wave

Alignment was done by isolating a window around the T-waves, calculating a mean T-wave template and checking the cross correlation between each T-wave and the mean

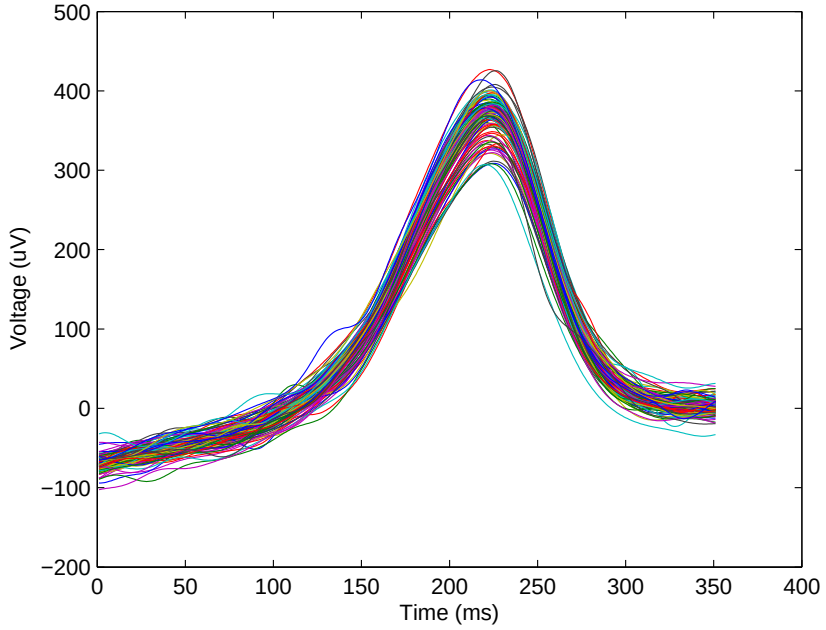

FIGURE 3.6: Aligned T-waves in one segment, 101 beats long. Values are recorded from Lead Y.

template.
The problem of this kind of procedure is that alternans may be touched as it is localized everywhere inside the wave.
Eventually, after the alignment operation, a series of aligned T-waves is obtained (see fig 3.6).

3.4.3 Median T-wave template extraction

Next step was to calculate a median T-wave template for odd beats and one for even beats, which was a necessary step in order to compute ADTWA index. This was done by isolating a window 100 ms after the QRS peak, 350 ms long and calculating two median templates, one for odd beats and one for even beats. Median operator was used as it is less sensitive to noise than the mean. Fig 3.7 shows, superimposed, two median T waves for even and odd beats, calculated in one segment. Fig 3.8 shows the median T wave in the same segment for all the beats.

3.5 Index computation

Next step was calculating the dominant T-Wave (t_D) and the vector of lead factors ($|\lambda_e u_e - \lambda_o u_o|$) for every analyzed segment, as described in 2.6.3. Then the following indexes have been calculated:

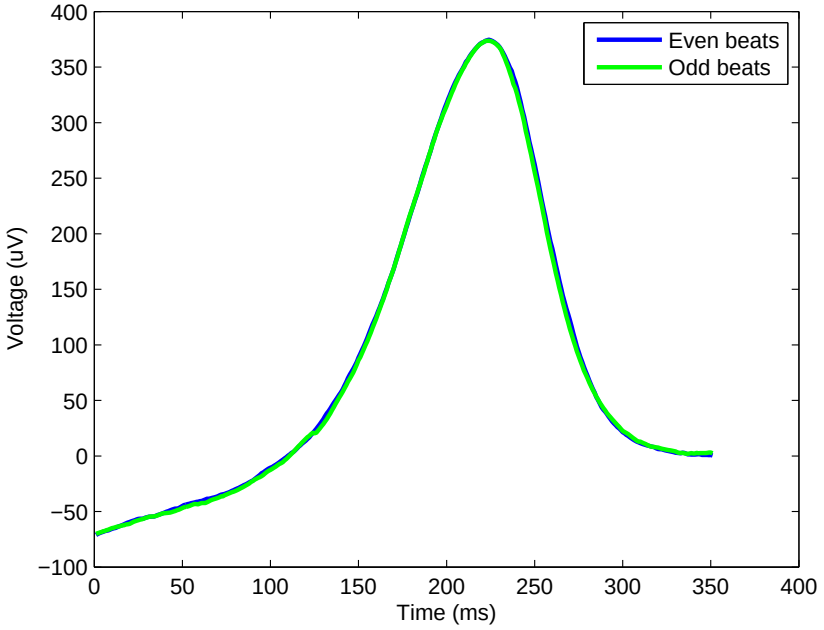

FIGURE 3.7: Median T-waves for even beats (blue waveform) and for odd beats (green waveform). Same segment of fig 3.6 was considered.

- **ADTWAI** : *Amplitude of Dominant T-Wave Alternans Index*
  Mean TWA activity evaluated during the whole ECG recording.

- **ADTWAI** evaluated for specific HR bins:
  - **ADTWAI70** : Represents the mean TWA activity evaluated only in segments whose mean HR is comprised between **60 and 70 bpm**.
  - **ADTWAI80** : Represents the mean TWA activity evaluated only in segments whose mean HR is comprised between **70 and 80 bpm**.
  - **ADTWAI90** : Represents the mean TWA activity evaluated only in segments whose mean HR is comprised between **80 and 90 bpm**.
  - **ADTWAI100** : Represents the mean TWA activity evaluated only in segments whose mean HR is comprised between **90 and 100 bpm**.
  - **ADTWAI110** : Represents the mean TWA activity evaluated only in segments whose mean HR is comprised between **100 and 110 bpm**.

The same analysis as Monasterio et al. [24] were repeated, plotting the boxplots of the alternans indexes (ADTWAI, ADTWAI70, ADTWAI80, ADTWAI90, ADTWAI100, ADTWAI110).
Each of the indexes has been evaluated with three different methods, which will be described in the following paragraphs.

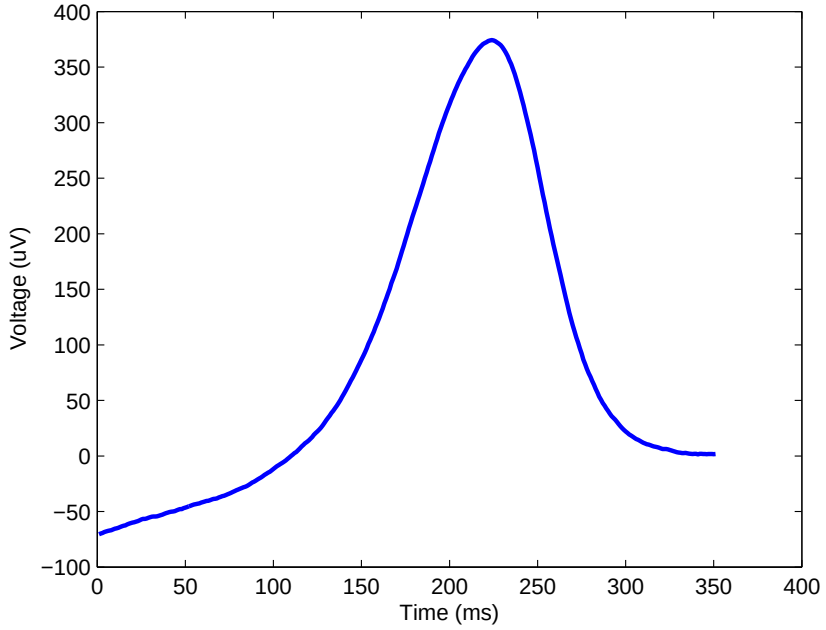

FIGURE 3.8: Median of all the T-waves represented in fig 3.6.

3.5.1 AM Method

In **AM Method** (*Average of Maximum*) the following steps are followed:

I One segment is kept good for analysis;

II On that segment, beats are aligned - with respect to the T wave or to the QRS complex -, then two median templates are calculated - one for odd beats, the other for even beats;

III Steps described in paragraph 2.6.3 are followed and the index I of ADTWA is calculated in this way : $\max_l |\lambda_e u_e - \lambda_o u_o| \max_t |t_D|$ (see eq. 2.9) ;

IV Procedure is repeated for the next segment valid for analysis;

V Eventually a global average of the calculated indexes is done.

Clearly this kind of method produces values more influenced by noise: in fact it resulted in the least significant result we were able to get. Nevertheless it had been useful to get a first graphical glimpse of alternans during the whole recording. As a matter of fact, the trend of TWA to grow at higher HR is evident and confirmed from the first order regression analysis for almost all the subjects.

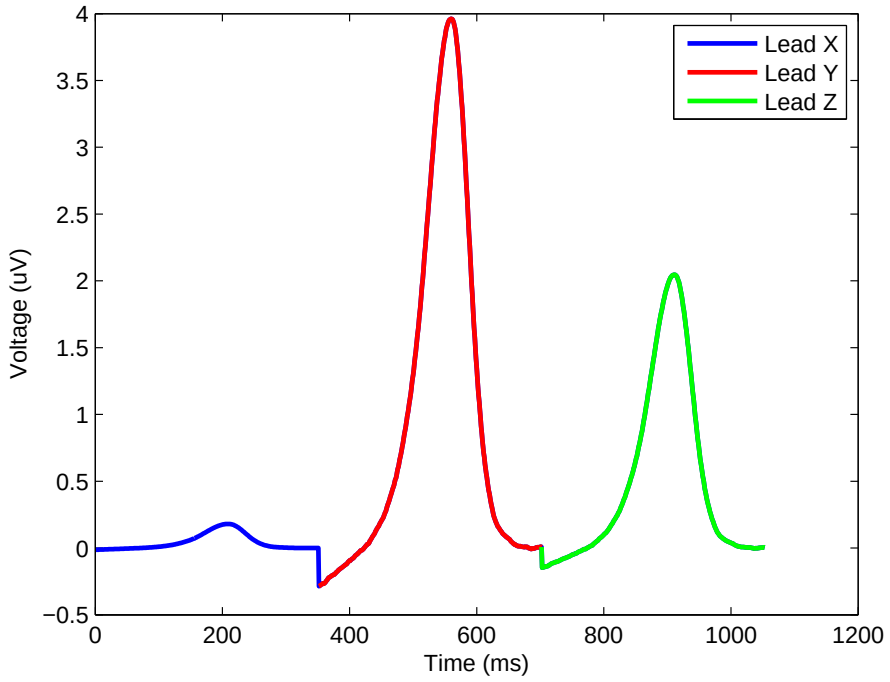

FIGURE 3.9: T Wave Alternans waveform for a single segment. Values recorded from Lead X are shown in blue, values from Lead Y are shown in red and values from Lead Z are shown in green.

3.5.2 MM Method

In **MM Method** (*Maximum of Mean*) a T-wave alternans waveform is computed which is the vector of lead factors multiplied for the dominant T-wave *in that segment*:

$$(\lambda_e u_e - \lambda_o u_o) * t_D \tag{3.1}$$

An example is shown in fig 3.9. The algorithm puts together values recorded from the three orthogonal leads in the same vector, thus waveforms from Lead X, Lead Y and Lead Z are shown together in the same graph. Procedure is repeated and a waveform of alternans is kept for every valid segments. The result is a matrix X, whose dimensions are $[3MXN]$, where M = 350 is the length of the T-wave window and N is the number of segments kept for analysis. Fig 3.10 shows the plot of the alternans waveforms during the whole recording.

Waveforms presenting a negative correlation with the cross correlation matrix X*X' are multiplied for -1. Otherwise, waveforms out of phase would collapse when the mean is done, producing falsely low values of alternans.

Finally, the absolute value of the mean of all the waveforms is calculated and its maximum is taken as an index of alternans.

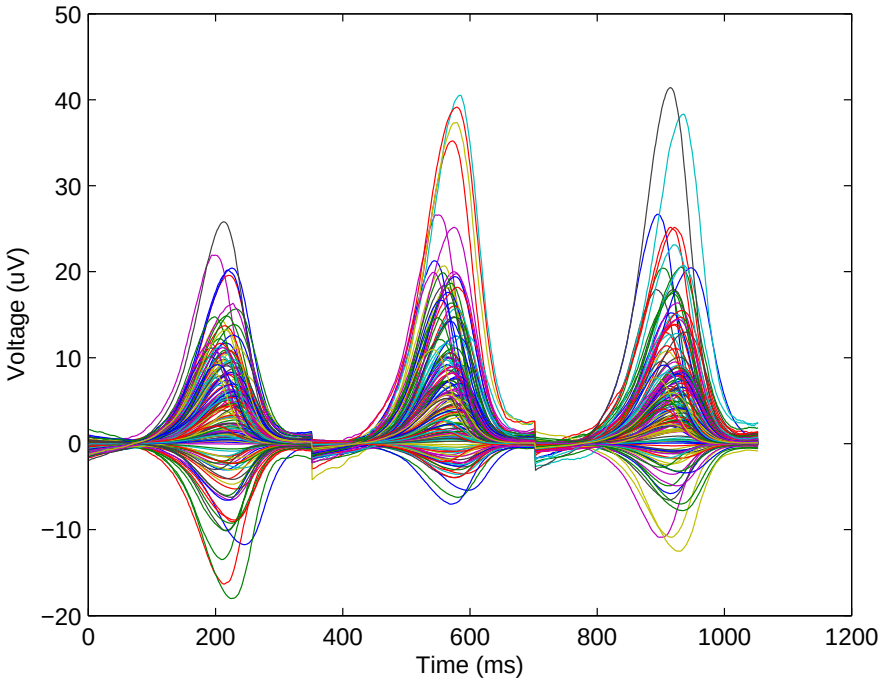

FIGURE 3.10: Alternans waveforms during the 24 hours. The alternans waveforms on each lead are shown together.

In fig 3.11 an example of mean ADTWA waveform for one subject is shown. The red dot represents the ADTWAI2 value for that subject.

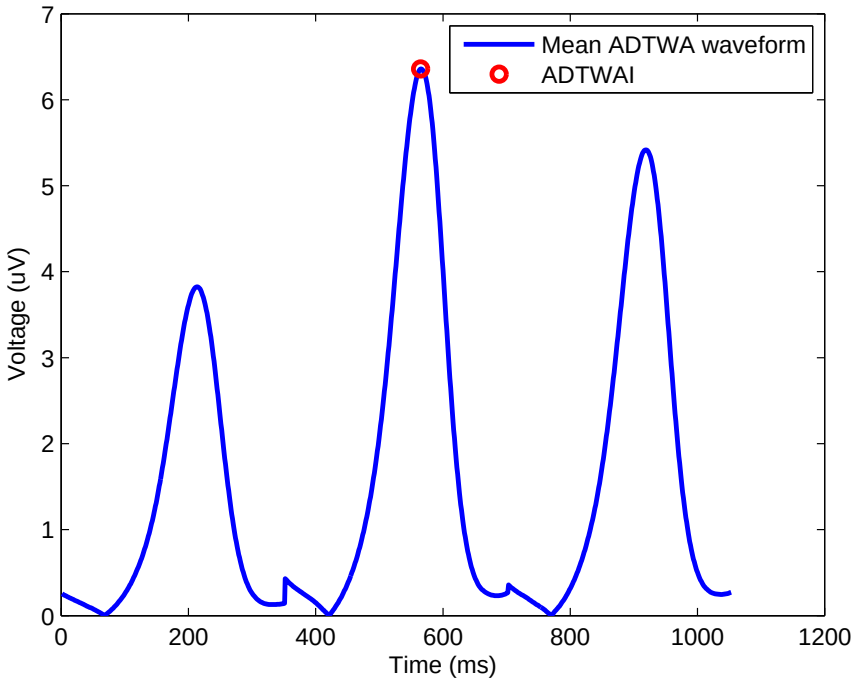

FIGURE 3.11: ADTWAI2 calculation. The thick blue line represents the absolute value of the mean waveform for one subject during the 24 hours. The red dot is the ADTWAI2 value, which is the maximum value of the absolute value of the mean waveform.

3.5.3 VM Method

In **VM method** (*Vectorcardiogram Maximum*), as in MM Method, waveforms of alternans are calculated and averaged during all the 24 hours or only for specific heart rhythms for each lead X,Y,Z (see fig. 3.12).

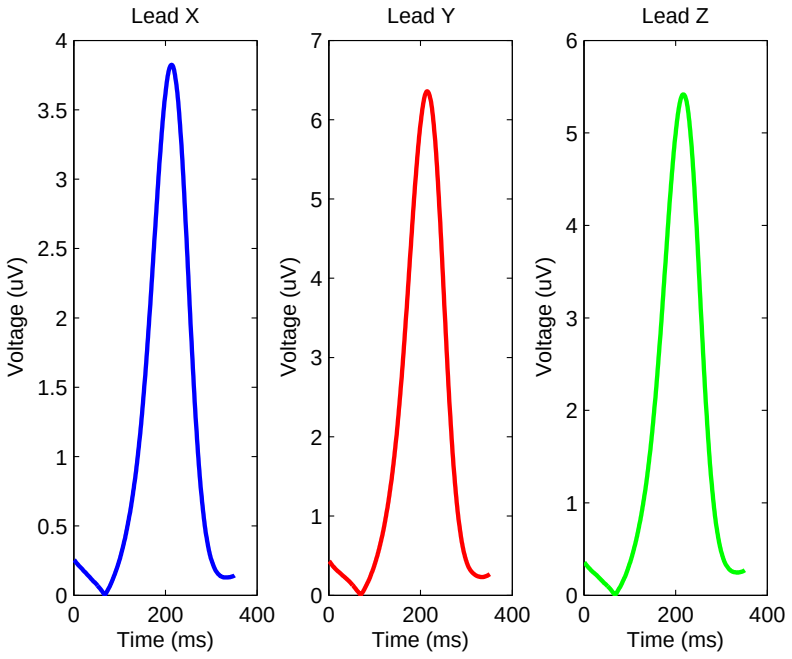

FIGURE 3.12: Alternans waveforms on leads X,Y,Z.

Then, the vectorcardiogram (VCG) magnitude is calculated in this way (see fig: 3.13).

$$VCG = \sqrt{X^2 + Y^2 + Z^2} \tag{3.2}$$

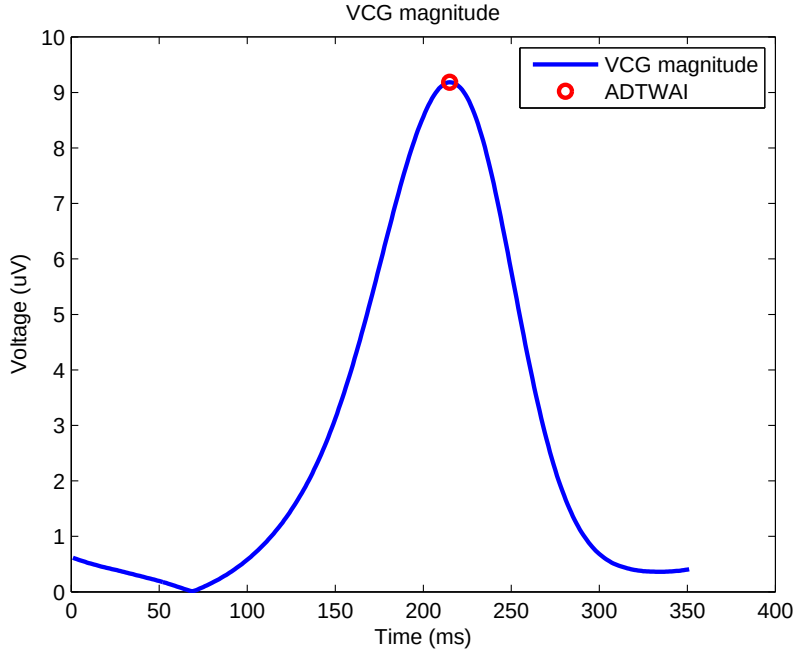

FIGURE 3.13: VCG magnitude and value of ADTWA recorded with VM Method (red dot).

Finally, the maximum is taken in this waveform as an index of alternans.
The measurement of alternans through this method has a clear *physiological meaning*. In fact, as already discussed in paragraph 1.1.4, the **vectorcardiogram** is the *spatial projection* of the electrical activity of the heart in three different directions. The resulting information is global, as it takes into account values recorded in all the three leads.

3.6 Statistical analysis

3.6.1 Boxplots

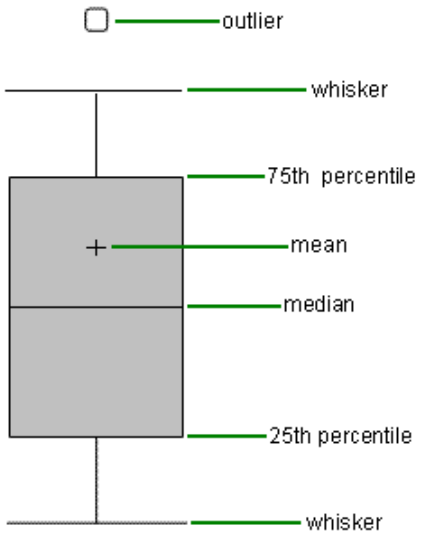

FIGURE 3.14: An example of boxplot. 25th percentile, median, mean, 75h percentile, whiskers and one outlier are shown for a sample distribution.

Boxplots are non parametric graphs displaying variations in samples of a statistical population. They generically represent the *25th percentile* (first edge of the box), the *median* (center of the box), the *75th percentile* (second edge of the box) and the *most extreme datapoints* which are not considered to be outliers (whiskers of the box). Outliers are plotted individually.
An example is shown in fig. 3.14.

3.6.2 Roc curves

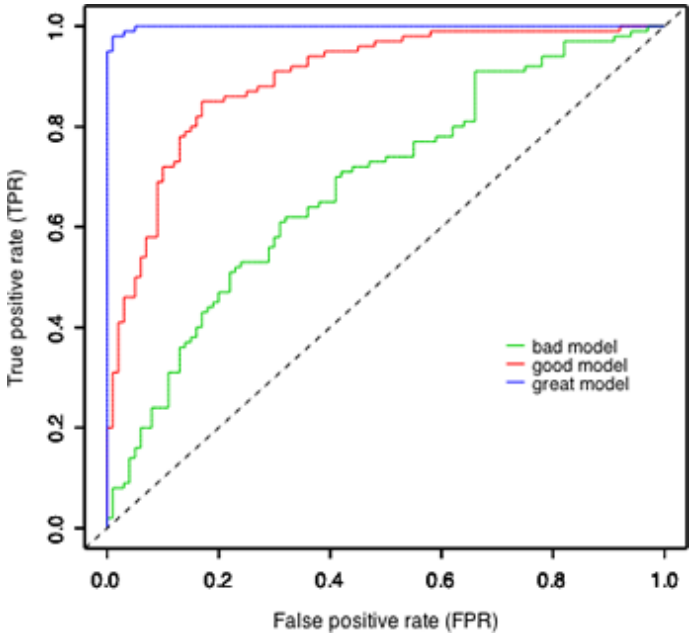

FIGURE 3.15: An example of Roc Curve. Three binary classifiers are shown and the straight line $sensitivity = (1 - specificity)$ is represented as well. The optimal model is the one which presents the larger area under the ROC Curve (AUC).

The ROC curve is a fundamental tool for diagnostic test evaluation. It is a graphical plot which illustrates the performance of a binary classifier system as its discrimination threshold is varied. In a ROC curve the true positive rate (*Sensitivity*) is plotted as a function of the false positive rate (*1 - Specificity*) for different cut - off points of a parameter. Each point on the ROC curve represents a sensitivity/specificity pair corresponding to a particular decision threshold.
Plotting Roc curves presents two fundamental advantages:

- The area under the ROC curve (AUC) is a measure of how well a parameter can distinguish between two diagnostic groups (diseased/normal).
- An optimal cut - off value to distinguish positives and negatives to a clinical test may be found by visually inspecting the shape of the curves.

An example of Roc Curve is plotted in fig 3.15.

3.6.3 Kaplan Meier survival analysis

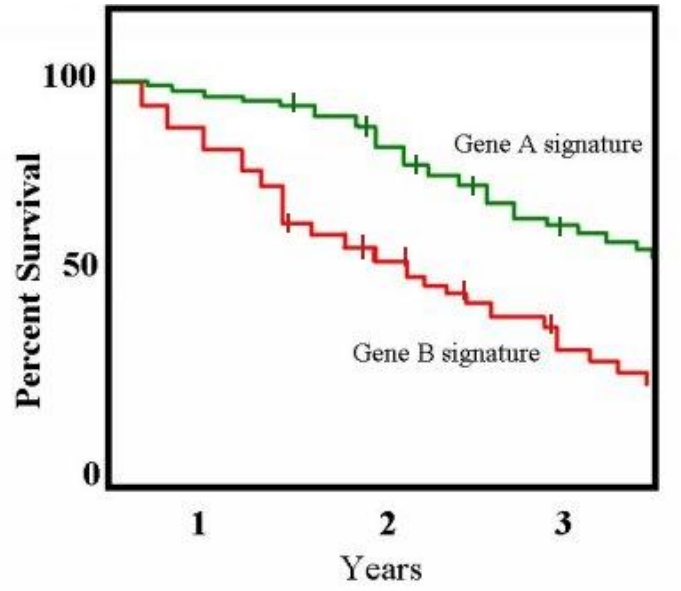

FIGURE 3.16: An example of Kaplan Meier survival analysis. The cumulative survival of two populations with different gene signatures (Gene A and Gene B) is compared.

Kaplan Meier estimator, also known as the product limit estimator, is used to estimate the survival function of data related to life duration. In medical research, it is often used to estimate the fraction of patients who live for a certain amount of time after the treatment.
A graph of the Kaplan Meier estimate of the survival function is a series of horizontal steps with decreasing amplitude which, if the used sample is sufficiently big, approximate the true survival function for that population.
An important advantage of Kaplan-Meier curve is that the method can take into account some types of censored data, in particular right censoring, which happens when a patients withdraws from the study, that is if he retires from the sample before final outcome can be observed.
When a right censoring happens, this is indicated in the diagram with a vertical tick. When no censoring or truncation occurs, the Kaplan Meier curve is the complement of the empirical distribution function.
In medical statistics, a typical application implies grouping patients in categories, such as patients with two different profiles. In fig 3.16 an example is shown, which compares the survival percentage of two groups of patients with different gene signatures.

3.6.4 Student's *t*-test

A *t-test* is a statistical hypothesis test which can be applied to data following a Student's t distribution. It is mostly applied to determine if two populations are significantly

different from each other. In fact, when a t-test is done, the null hypothesis is that the means of the two groups are equal. These tests are often referred to as "*unpaired*" or "*independent samples*" t-tests, as they are typically applied when the statistical units underlying the two samples being compared are non-overlapping.
We used Student's t-test in order to compare the distribution of ADTWA in the group of people who survived during the follow - up phase with the group of people who died from SCD.

3.6.5 Log - Rank Test

Log - Rank Test is an hypothesis test used to verify the survival functions of two populations. It is a non parametric test which can only be used if data are asymmetrical and right - censored. It is widely used in clinical tests in order to asset a new treatment's efficacy when compared to a control treatment when time preceding an event (such as time between initial treatment and heart attack) is known. Sometimes it is called Mantel - Cox test.
We used Log - Rank Test in order to compare the survival functions of the group of subjects who presented a mean TWA activity below a certain threshold during all hours of record ($ADTWA$ - *negatives*) with the group of subjects whose mean TWA activity was above threshold ($ADTWA$ - *positives*).

3.6.6 Software used

ECG analysis was performed using self written Matlab® functions.
The processing of one single ECG required an approximate time of two hours, thus processing in series all the database would have required an excessive amount of time. Process was greatly sped up by using the HERMES supercomputing center, used by I3A researchers, equipped with more than 1500 computing cores, which allowed to process the whole database in slightly more than 45 minutes.
Statistical analysis has been done using IBM® SPSS® Statistics 20.

Chapter 4

Materials

4.1 Study population (MUSIC)

In this study MUSIC (*MUerte Súbita en Insuficiencia Cardiaca*) database [34] has been used. MUSIC study is a prospective work realized in patients enrolled in 9 centers in Spain between April 2003 and December 2004 who suffered from symptomatic heart failure (CHF, II-III NYHA functional classes). The study was designed to assess risk predictors for cardiovascular mortality in ambulatory patients with CHF.
Specific enrollment criteria for the MUSIC Study included CHF symptoms more than 3 months after last hospitalization due to heart failure decompensation and at least one of the following echocardiographic sign of systolic and / or diastolic disfunction:

- Left ventricle ejection fraction $< 40\%$;
- Diastolic diameter over $60mm$;
- Left ventricular hypertrophy (sept or posterior wall thickness over $14mm$);
- Abnormal relaxation patterns characteristic for diastolic dysfunction.

The exclusion criteria were as follows:

- Heart failure secondary to an acute reversible cause in patients with no prior history of heart failure (e.g. hyperthyroidism);
- Heart failure secondary to valvular heart disease amenable to surgical repair;
- Right ventricular heart failure associated with chronic col pulmonale or concomitant terminal disease.

4.1.1 Patients characteristics

992 ambulatory patients with CHF were included in the MUSIC study (718 men and 274 women), aged 18-89 years (mean 65 ± 12). Most patients (78.4%) were in NYHA class II. A detailed resume of the characteristics of the population studied can be found in Table 4.1.

4.2 Study protocol

The study protocol was approved by institutional Investigation Committees and all patients signed informed consent.
First assessments were performed in 1054 patients; 58 were not included due to poor acoustic windows and 4 additional patients refused to give their consent for the study. MUSIC population was made by the remaining patients (992) and for our analysis we only considered a subset of 650 cases which presented sinus rhythm.
12-lead ECGs with a sampling rate of 200 Hz were recorded using SpiderView recorders (ELA Medical, Sorin Group, Paris, France). All patients had echocardiography, chest X-Ray, 24 hours Holter monitoring and blood laboratory parameters performed at enrollment.
As far as the follow-up phase is concerned, visits were conducted on an outpatient basis every 6 months, for a median of 44 months. By asking patients' physicians and relatives or investigating medical records, the attempt was made to determine the cause of death. The total number of recorded deaths was 267 (26.9%), the most part of which had a cardiovascular origin (213). Among these ones, 123 (12.4%) were due to **pump failure** (PF) and 90 (9.1%) due to **sudden cardiac death** (SCD).
Death was defined as '*sudden*' in any of these three cases:

- A witnessed death occurring within one hour from the onset of new symptoms, unless a non cardiac cause was evident;
- An unwitnessed death ($24h$) in the absence of pre-existing progressive circulatory failure or other causes of death;
- A death during attempted resuscitation.

Some patients were lost to follow-up (n = 11) and censored in survival analysis. Those who underwent cardiac transplantation (n = 20) were defined as PFD at the time of surgery.

Demographic and clinical variables	
Age, years	65±12
Gender, male	718 (72.4%)
Diabetes mellitus	356 (35.9%)
History of hypertension	565 (57.0%)
History of dyslipemia	494 (49.8%)
Current smoker	104 (10.5%)
Ischaemic aetiology	453 (45.7%)
Prior AVE	478 (48.2%)
Prior CABG or PTCA	256 (25.8%)
Prior pacemaker	135 (13.6%)
Body mass index, kg/m^2	28.5±4.5
NYHA class II	778 (78.4%)
NYHA class III	214 (21.6%)
Systolic blood pressure, $mmHg$	127±22
Radiographic variables	
Cardiothoracic ratio	0.55±0.07
Signs of pulmonary venous hypertension	169 (17.0%)
Laboratory variables	
Haemoglobin, g/L	137.2±15.9
GGT $> 50IU/L$	251 (25.3%)
Total cholesterol, $mmoL/L$	4.83 ± 1.07
Creatinine, $\mu mol/L$	109.1 ± 34.7
eGFR $< 60mL/min/1.73m^2$	458 (46.2 %)
Hyponatremia $\leq 138mEq/L$	374 (37.7 %)
NT-proBNP $> 1000ng/L$	452 (45.6 %)
Troponin - positive	158 (15.9 %)
Echocardiographic variables	
La size $> 26mm/m^2$	323 (32.6 %)
LV end-diastolic diameter, mm/m^2	32.8 ± 6.1
LV mass, g/m^2	162.4 ± 52.2
LVEF, %	37.0 ± 14.1
LVEF $< 45\%$	748 (75.4%)
LVEF $\leq 35\%$	534 (53.8 %)
Restrictive filling pattern	78 (7.9 %)
12-Lead ECG and 24-h Holter monitoring variables	
Sinus rhythm	703 (70.9%)
Atrial fibrillation	191 (19.3%)
Pacemaker rhythm	98 (9.9%)
Heart rate, *b.p.m.*	70.1 ± 10.1
QRS duration, ms	125.5 ± 35.1
LBBB or IVCD	485 (48.9%)
Non-sustained VT	352 (35.5%)
Frequent VPBs (> 240 VPBs in 24h)	480 (48.4%)
Non-sustained VT and frequent VPBs	284 (28.6%)

TABLE 4.1: Baseline characteristics in 992 heart failure patients in the MUSIC study

Chapter 5

Results

Results of this Master's Thesis work are presented in this chapter.
At first indexes of alternans have been calculated separately for each patient. Then a statistical analysis has been done on the whole population under study to check the prognostic value of ADTWA1, ADTWA2 and ADTWA3 for sudden cardiac death.
First *boxplots* of alternans indexes have been plotted. The aim was to verify if a trend of alternans to grow at higher heart rates was visible at a naked eye for the population under study. Through the analysis of *ROC Curves* the best cut-off value for the index to predict SCD was checked. Finally patients have been separated into positives and negatives to our TWA test (ADTWA > cut off value). *Kaplan Meier survival functions* have been calculated and plotted, using cut-off values seen in ROC Curves, in order to check if there was a significant difference between the percentage of survivals in the two groups.
This chapter is organized as follows: boxplots, ROC curves and survival functions will be presented for each method, when alignment on QRS complex is done. Then, the same results will be shown when alignment on T-waves is done.
Last paragraph shows an analysis of the prognostic value of ADTWA when analysis is restricted to slow heart rates. Two indexes have been found to be predictive for SCD : ADTWAI70 and ADTWAI90.

5.1 QRS alignment

5.1.1 Analysis of alternans

Table 5.1 represents the median and the interpercentile range (25th percentile - 75th percentile) for the 650 cases analyzed, globally and for specific heart rate bins.
Boxplots for the three methods are shown in figures 5.1, 5.2 and 5.3.

	Global	**60-70**	**70-80**	**80-90**	**90-100**	**100-110**
AM Method	7.19 [5.87 ÷ 8.82]	6.19 [4.62 ÷ 8.55]	7.86 [5.88 ÷ 10.45]	9.81 [7.25 ÷ 12.91]	11.66 [8.60 ÷ 15.70]	12.47 [9.12 ÷ 17.66]
MM Method	4.16 [3.23 ÷ 5.47]	3.75 [2.72 ÷ 5.43]	4.85 [3.57 ÷ 6.57]	6.01 [4.36 ÷ 8.19]	7.63 [5.22 ÷ 10.83]	8.12 [6.08 ÷ 13.12]
VM Method	4.85 [3.89 ÷ 6.17]	4.40 [3.21 ÷ 6.22]	5.82 [4.14 ÷ 7.62]	7.08 [5.18 ÷ 9.95]	8.80 [6.18 ÷ 13.05]	9.97 [7.01 ÷ 15.20]

TABLE 5.1: Median of ADTWA values and ranges [25th percentile ÷ 75th percentile]. All values are expressed in microvolts.

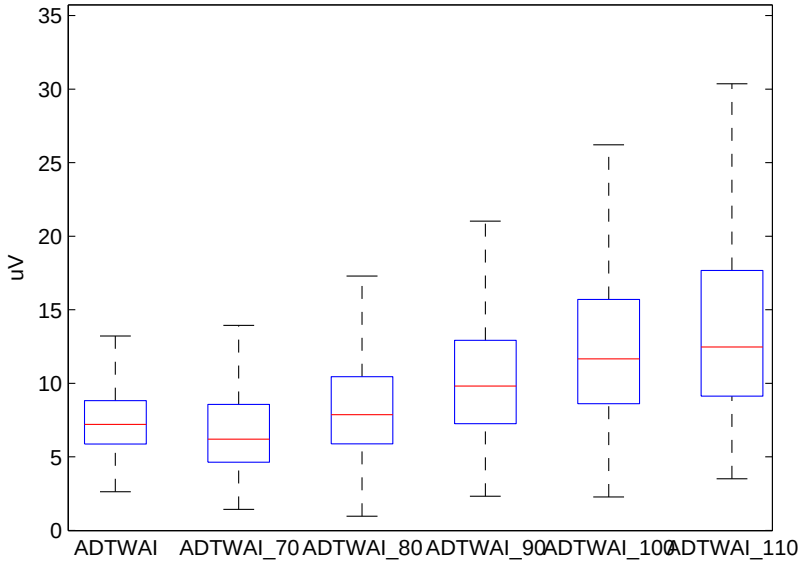

FIGURE 5.1: Boxplot of alternans indexes calculated with AM Method by aligning on QRS complex.

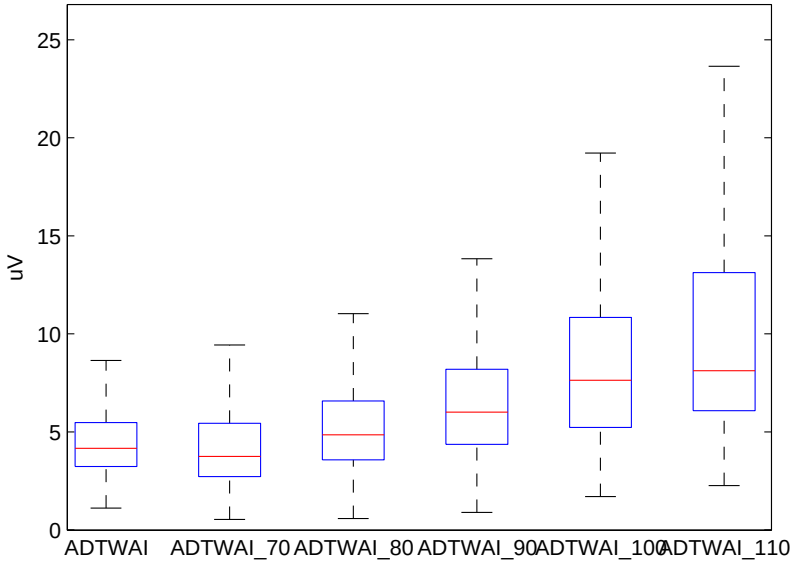

FIGURE 5.2: Boxplot of alternans indexes calculated with MM Method by aligning on QRS complex.

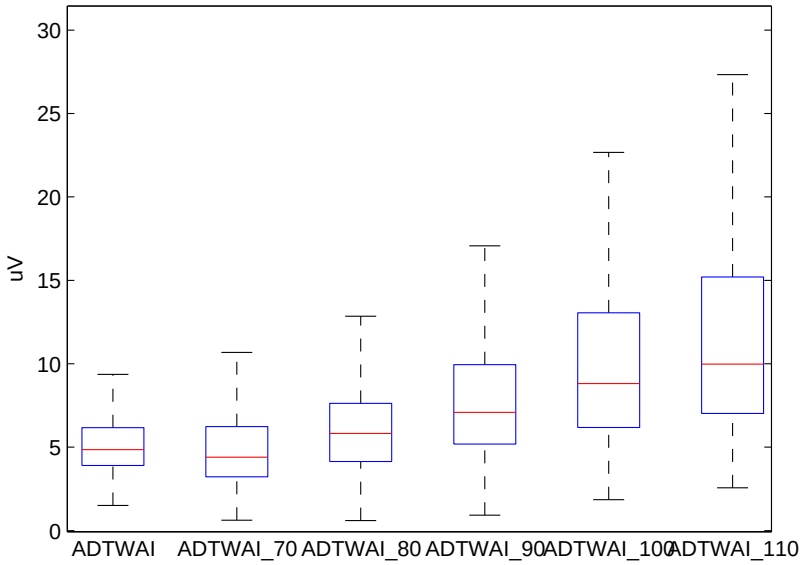

FIGURE 5.3: Boxplot of alternans indexes calculated with VM Method by aligning on QRS complex.

As expected, the distribution tends to be more spread out at higher heart rates. The trend was the same in all the three cases, but some differences can be highlighted:

- **AM Method** produced the highest values - as doing the average of the values on each segment results more sensitive to noise and motion artifacts thus producing higher values of alternans.
- **MM Method** produced the lowest values as keeping the waveforms and eventually doing a global average results in a lower sensitivity to noise.
- **VM Method** produced values which are slightly higher than those obtained from the second method, as computing the module of VCG consists in summing squared values from the three leads.

5.1.2 Survivors and SCD

Figure 5.4 shows the boxplot which compares the distribution of ADTWA in the two populations:

- People who survived (**Survivors**);
- People who died from Sudden Cardiac Death (**SCD**).

using VM Method, as example.

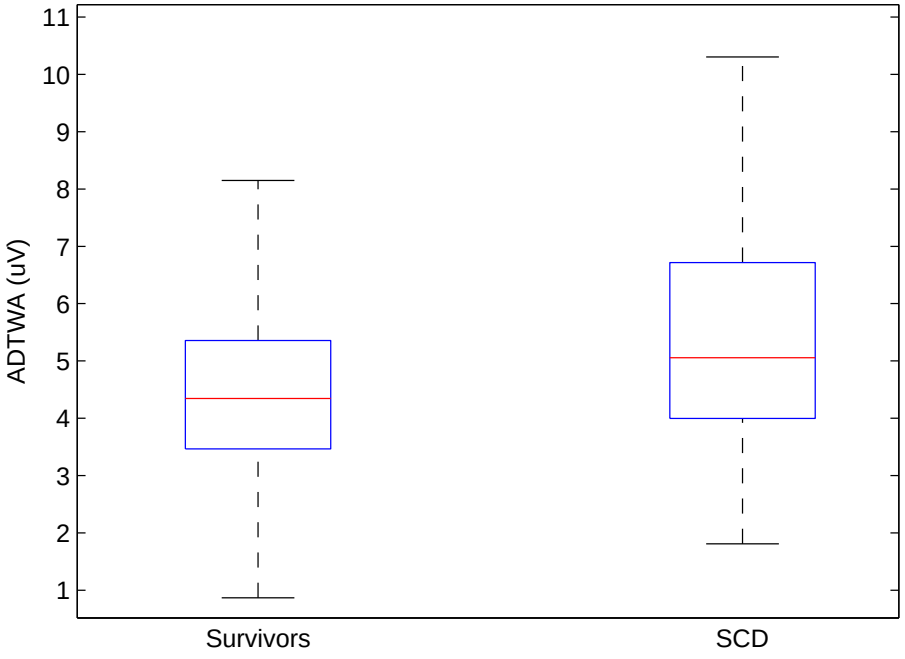

FIGURE 5.4: Boxplots comparing distribution of TWA in patients who survived during the follow-up phase (**Survivors**) and patients who died from SCD (**SCD**). ADTWA was calculated using VM Method and aligning beats on the QRS complex.

Tables 5.2 and 5.3 show, respectively, the **group statistics** for the two groups of subjects and the results of the **t - test**. A 2 - tailed significance of 0.01 was achieved under the assumptions of equal variances of the two groups, of 0.07 without that assumption.

	Mean	*N*	*Standard deviation*	*Std. error mean*
Survivors	4.59	504	1.71	0.08
SCD	5.43	52	2.08	0.29

TABLE 5.2: Statistic for the two populations of survivors and dead from SCD, as obtained when values are calculated with VM Method by aligning on QRS complex.

	t	*df*	*Sig (2-tailed)*	*Mean diff.*	*Std. Err. Diff.*
Equal variance assumed	-3.29	554	**0.01**	-0.84	0.25
Equal variance not assumed	-2.811	58.34	**0.07**	-0.84	0.3

TABLE 5.3: Indipendent Samples Test, as obtained when values are calculated with VM Method by aligning on QRS complex.

Figures 5.5,5.6 and 5.7 show the ROC curves for the three methods. The ROC curves were used to choose the best cut-off value for ADTWA, which is:

- $6.774\mu V$ for AM Method;
- $3.9328\mu V$ for MM Method;
- $4.7578\mu V$ for VM Method.

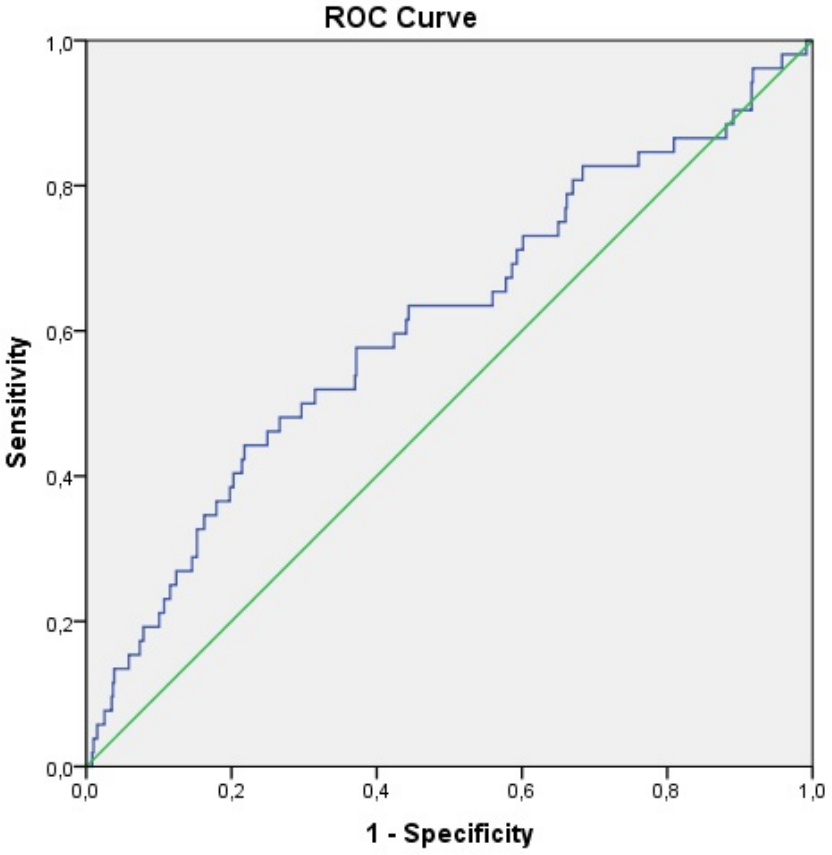

FIGURE 5.5: ROC Curve for AM Method with alignment on QRS complexes.

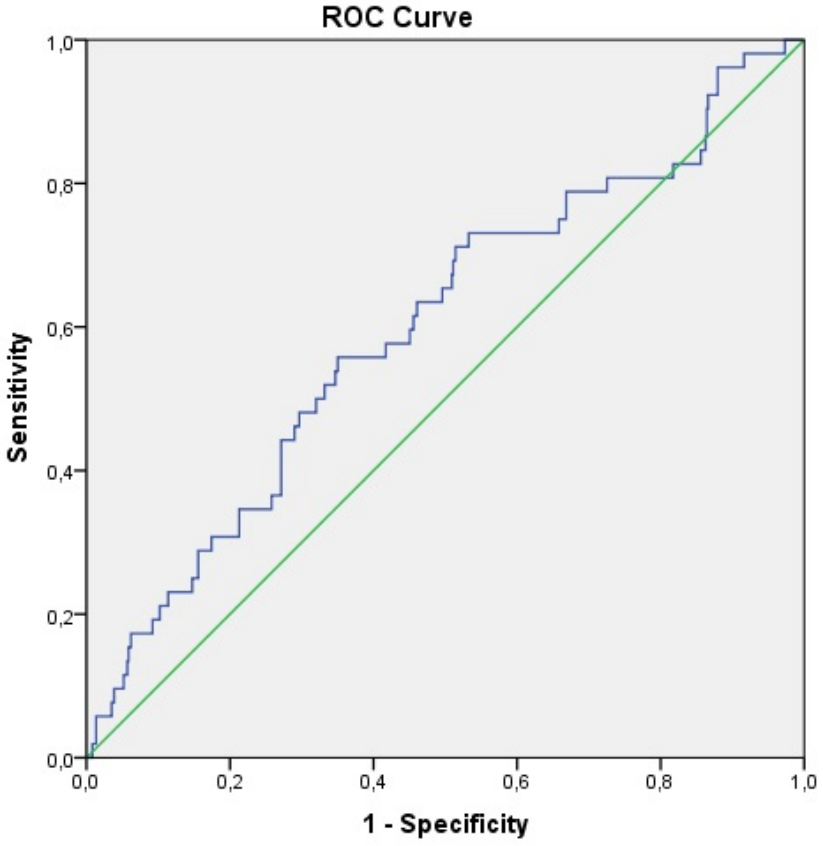

FIGURE 5.6: ROC Curve for MM Method with alignment on QRS complexes.

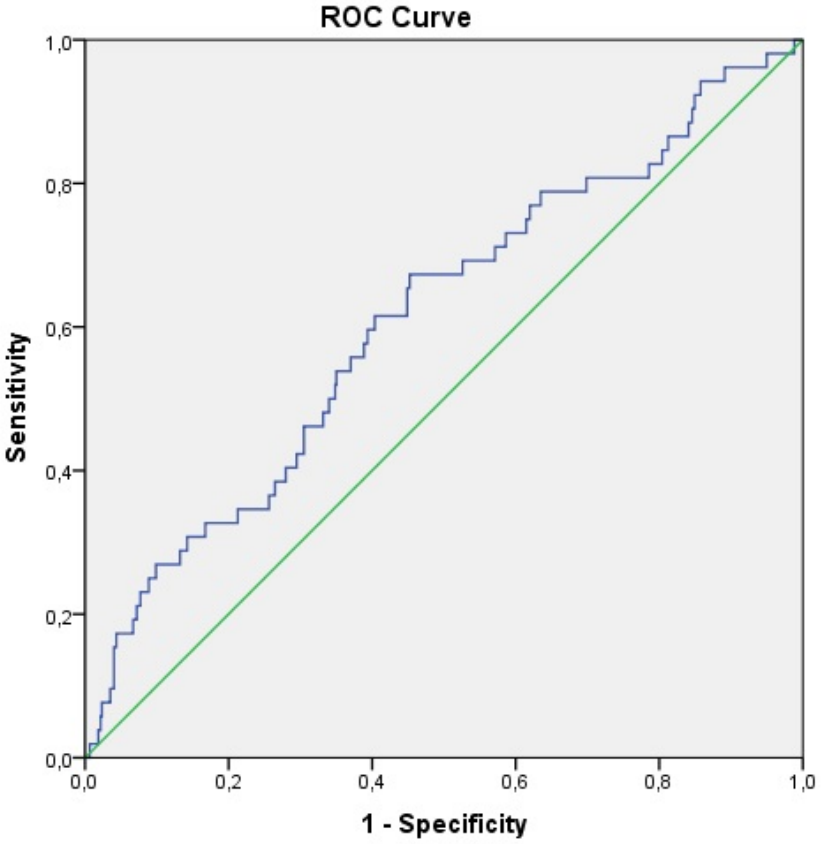

FIGURE 5.7: ROC Curve for VM Method with alignment on QRS complexes.

The cutoff values determined analyzing the ROC curves were used in the Kaplan Meier analysis. A mean TWA activity above a fixed threshold was used to discriminate the two populations (survivors vs SCD).
In figures 5.8, 5.9 and 5.10, cumulative survival is plotted as a function of time (days). Analysis has been restricted to 1440 days, i.e. almost 4 years.
The Log Rank test was used in order to check the statistical significance of the results. A significant difference was found using all three methods (p-values are reported in the figures caption).

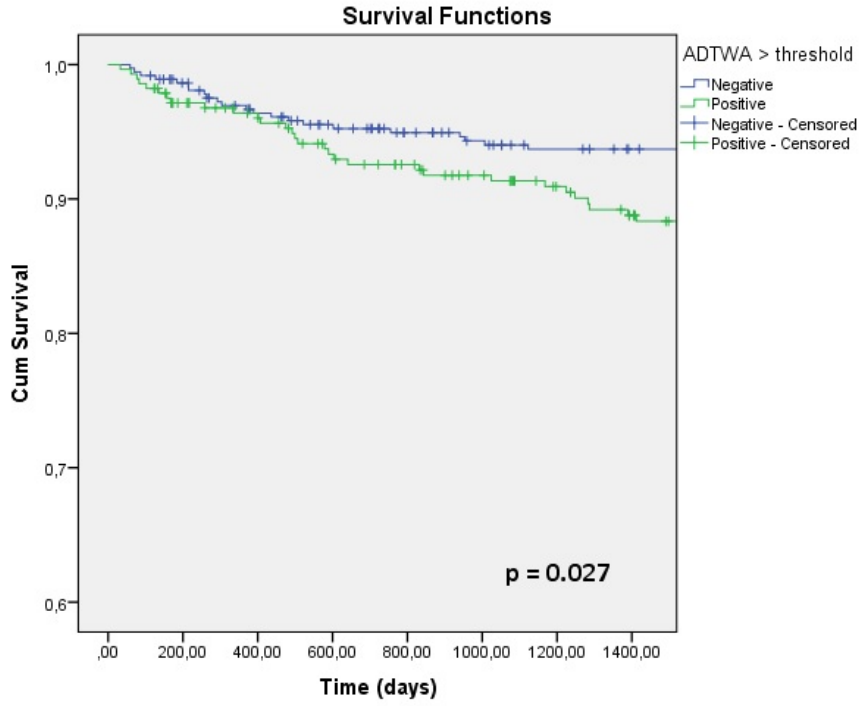

FIGURE 5.8: Kaplan Meier Survival Function for AM Method (ADTWA threshold = $6.774\mu V$)

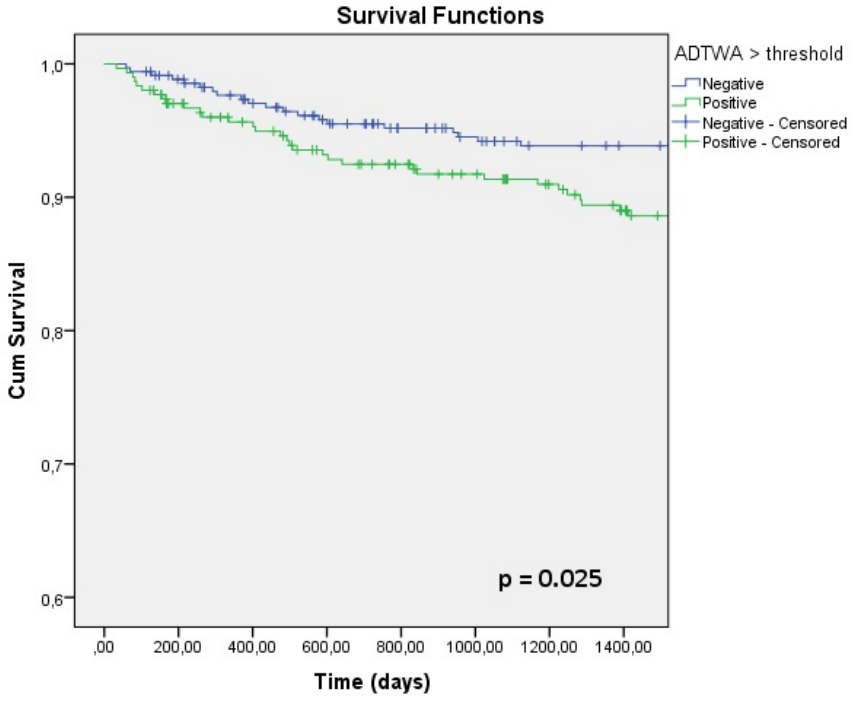

FIGURE 5.9: Kaplan Meier Survival Function for MM Method (ADTWA threshold = $3.9328\mu V$)

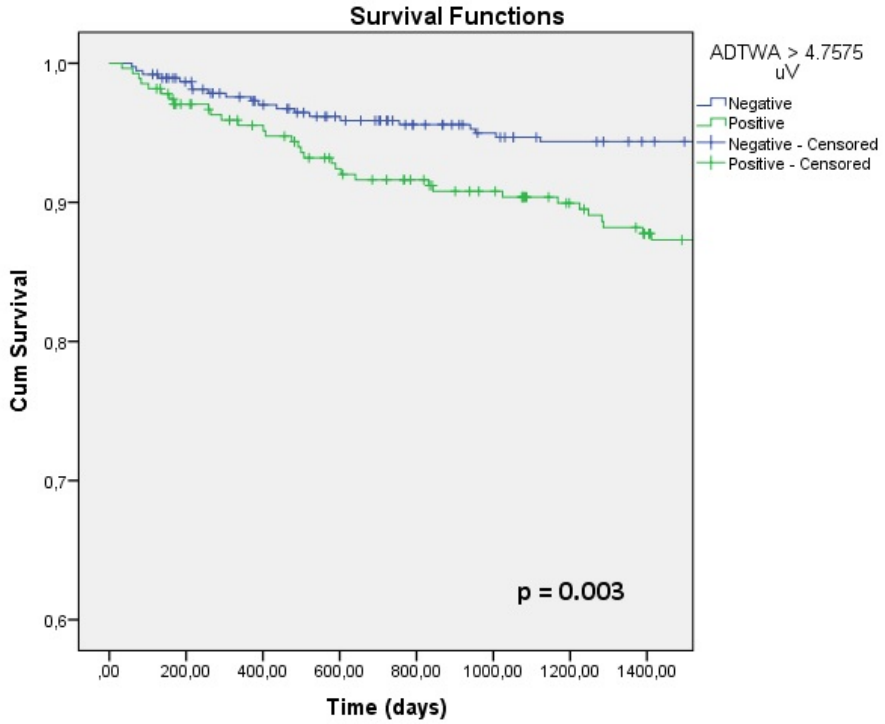

FIGURE 5.10: Kaplan Meier Survival Function for VM Method (ADTWA threshold = $4.7575\mu V$)

5.2 T-wave alignment

The same analysis have been repeated when alignment on T-waves is done. This was a "risky" approach as alternans may be localized everywhere in the ST-T segment and this kind of procedure may result in altered values of TWA. Nevertheless, values were found to be quite similar to the ones found with the previously described method and *box-plots* kept displaying a linear dependence of TWA on HR. Also in this case *Roc Curves* permitted to find optimal cut - off values to discriminate positives and negatives to our TWA test. *Kaplan Meier survival functions* produced graphs similar to the previous approach, even if we found slightly lower values of statistical significance.

5.2.1 Analysis of alternans

Table 5.4 represents the median and the interpercentile range (25th percentile - 75th percentile) for the 650 cases analyzed, globally and for specific heart rate bins.

	Global	**60-70**	**70-80**	**80-90**	**90-100**	**100-110**
AM Method	6.78 [5.81 ÷ 7.98]	5.98 [4.81 ÷ 7.65]	7.18 [5.69 ÷ 8.58]	9.81 [6.99 ÷ 10.64]	9.88 [7.48 ÷ 12.54]	10.75 [7.32 ÷ 13.45]
MM Method	3.87 [3.14 ÷ 4.96]	3.72 [2.87 ÷ 4.97]	4.42 [3.26 ÷ 5.60]	5.59 [4.28 ÷ 7.08]	6.29 [4.72 ÷ 9.04]	7.08 [4.55 ÷ 12.05]
VM Method	4.59 [3.70 ÷ 5.59]	4.32 [3.31 ÷ 5.64]	5.82 [3.80 ÷ 6.40]	6.33 [4.96 ÷ 8.28]	7.02 [5.34 ÷ 10.79]	8.05 [5.67 ÷ 13.92]

TABLE 5.4: Median of ADTWA values and ranges [25th percentile ÷ 75th percentile].

Boxplots for the three methods are shown in figures 5.11, 5.12 and 5.13.

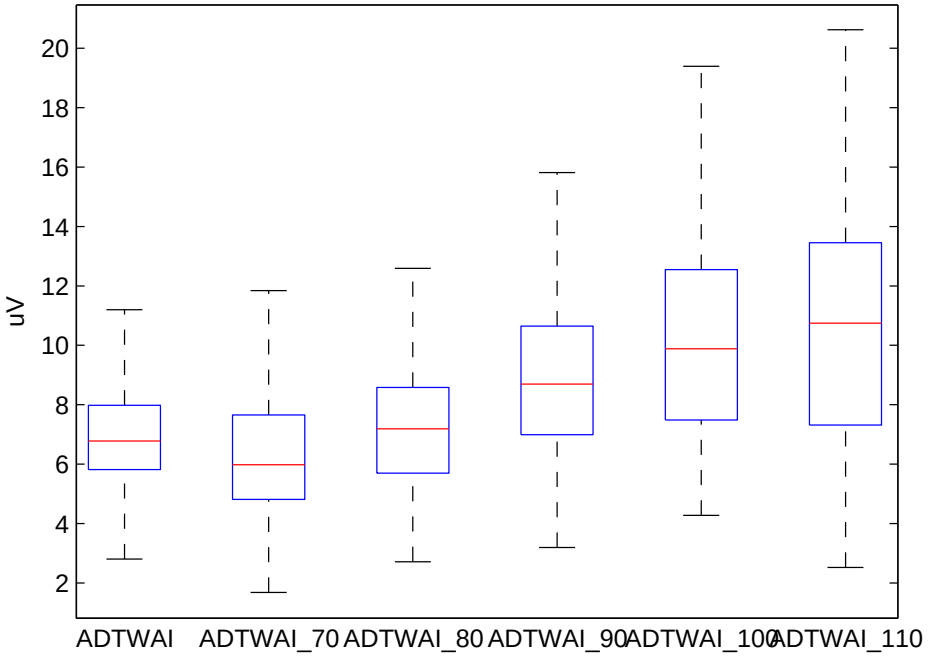

FIGURE 5.11: Boxplot of alternans indexes calculated with AM Method by aligning on T wave.

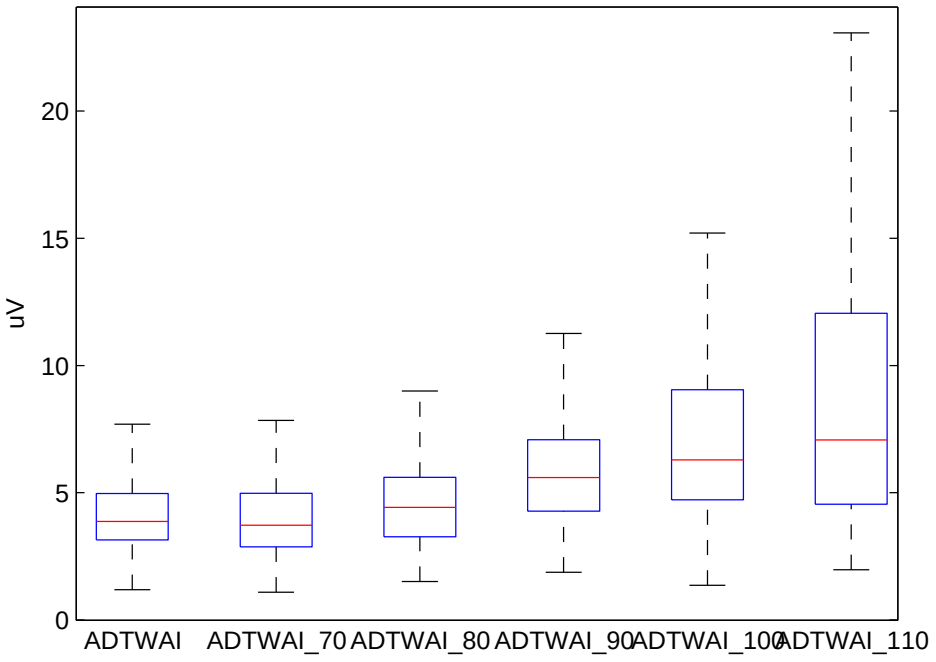

FIGURE 5.12: Boxplot of alternans indexes calculated with MM Method by aligning on T wave.

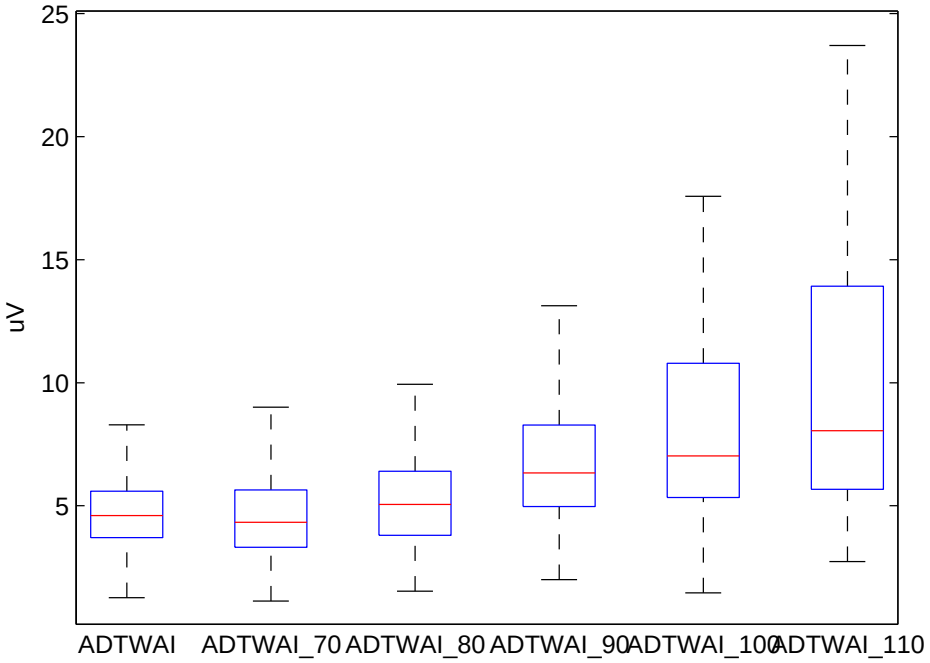

FIGURE 5.13: Boxplot of alternans indexes calculated with VM Method by aligning on T wave.

5.2.2 Survivors and SCD

Figure 5.14 shows the boxplot which compares the distribution of ADTWA in the two populations:

- People who survived (**Survivors**);
- People who died from Sudden Cardiac Death (**SCD**).

using VM Method, as example.

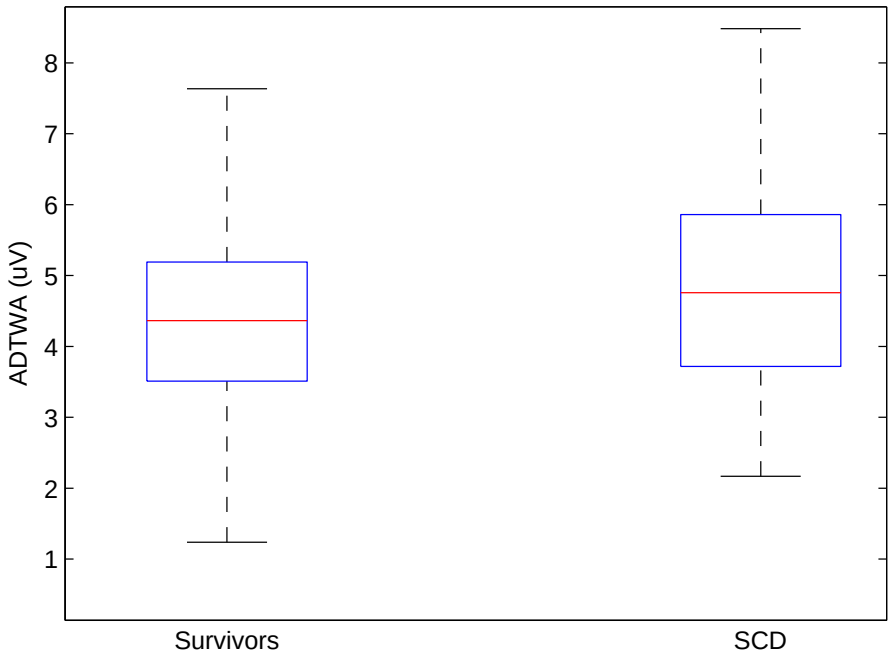

FIGURE 5.14: Boxplots comparing distribution of TWA in patients who survived during the follow-up phase (**Survivors**) and patients who died from SCD (**SCD**). ADTWA was calculated using VM Method and aligning beats on the T wave.

Tables 5.5 and 5.6 show, respectively, the **group statistics** for the two groups of subjects and the results of the **t - test**. In this case, difference between the two groups did not reach statistical significance (p >, 0.05).

	Mean	*N*	*Standard deviation*	*Std. error mean*
Survivors	4.67	503	2.08	0.92
SCD	5.06	53	1.93	0.26

TABLE 5.5: Statistic for the two populations of survivors and dead from SCD, as obtained when values are calculated with VM Method by aligning on T wave.

	t	*df*	*Sig (2-tailed)*	*Mean diff.*	*Std. Err. Diff.*
Equal variance assumed	-1.43	557	0.152	-0.43	0.30
Equal variance not assumed	-1.53	65.33	0.132	-0.43	0.28

TABLE 5.6: Indipendent Samples Test, as obtained when values are calculated with VM Method by aligning on T wave.

Figures 5.15,5.16 and 5.17 show the ROC curves for the three methods. The ROC curves were used to choose the best cut-off value for ADTWA, which is:

- $6.81\mu V$ for AM Method;
- $3.8024\mu V$ for MM Method;
- $4.4751\mu V$ for VM Method.

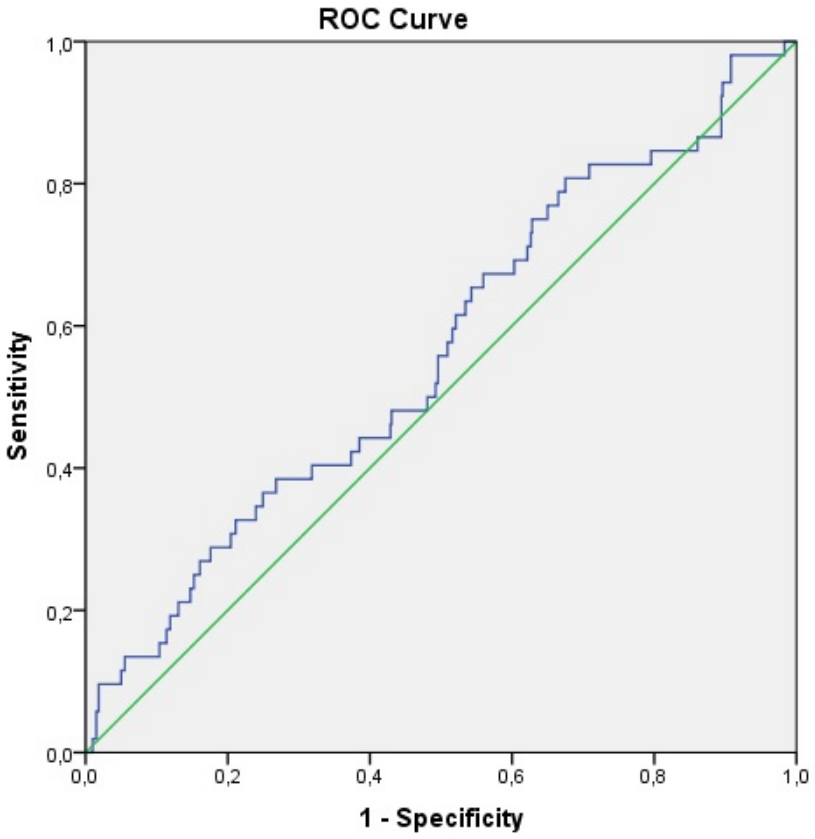

FIGURE 5.15: ROC Curve for AM Method when alignment on T-wave is done.

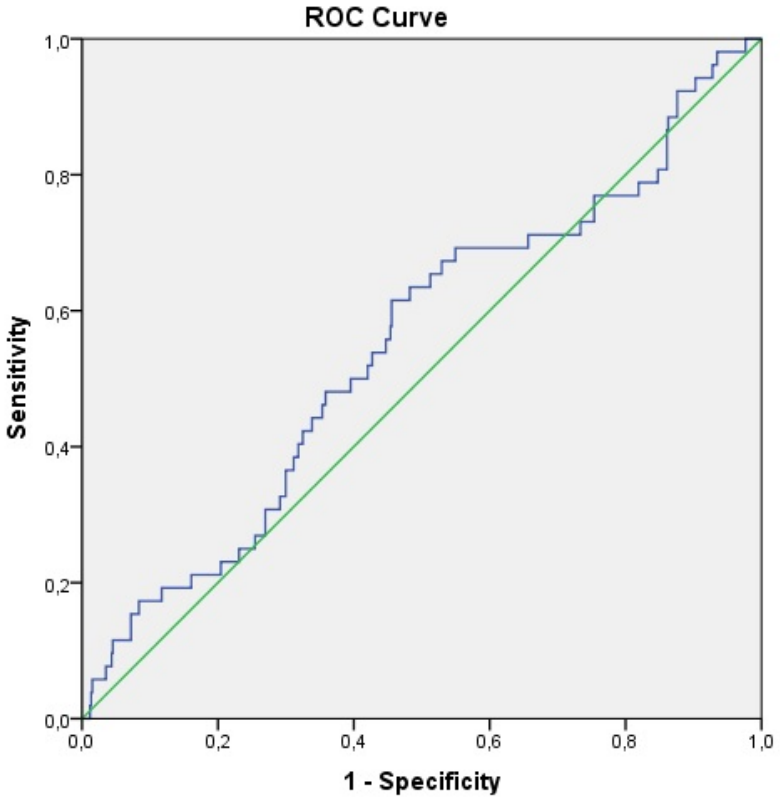

FIGURE 5.16: ROC Curve for MM Method when alignment on T-wave is done.

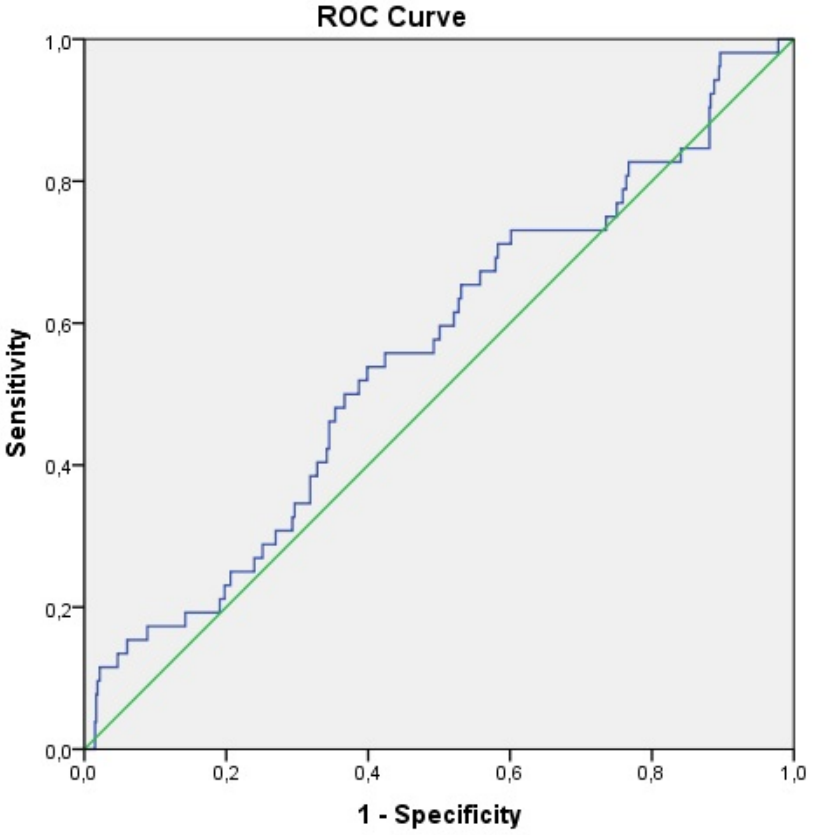

FIGURE 5.17: ROC Curve for VM Method when alignment on T-wave is done.

The cut - off values determined analyzing the ROC curves were used in the Kaplan Meier analysis. A mean TWA activity above a fixed threshold was used to discriminate the two populations (survivors vs SCD). In figures 5.18, 5.19 and 5.20, cumulative survival is plotted as a function of time (days).
Analysis has been restricted to 1440 days, i.e. almost 4 years.
The Log Rank test was used in order to check the statistical significance of the results. A significant difference was found using all three methods (p-values are reported in the figures caption).

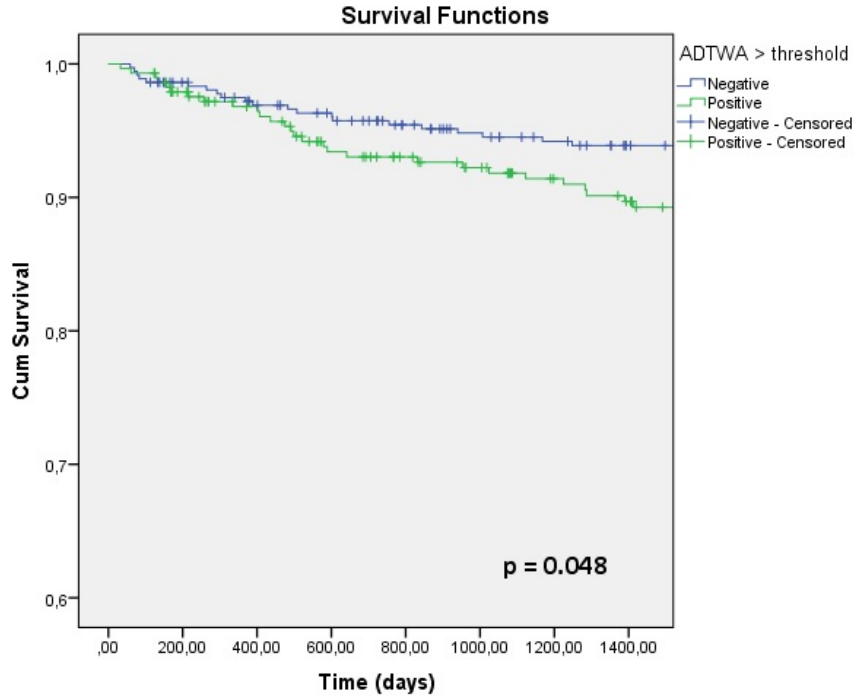

FIGURE 5.18: Kaplan Meier Survival Function for AM Method when alignment on T-wave is done (ADTWA threshold = $6.81\mu V$)

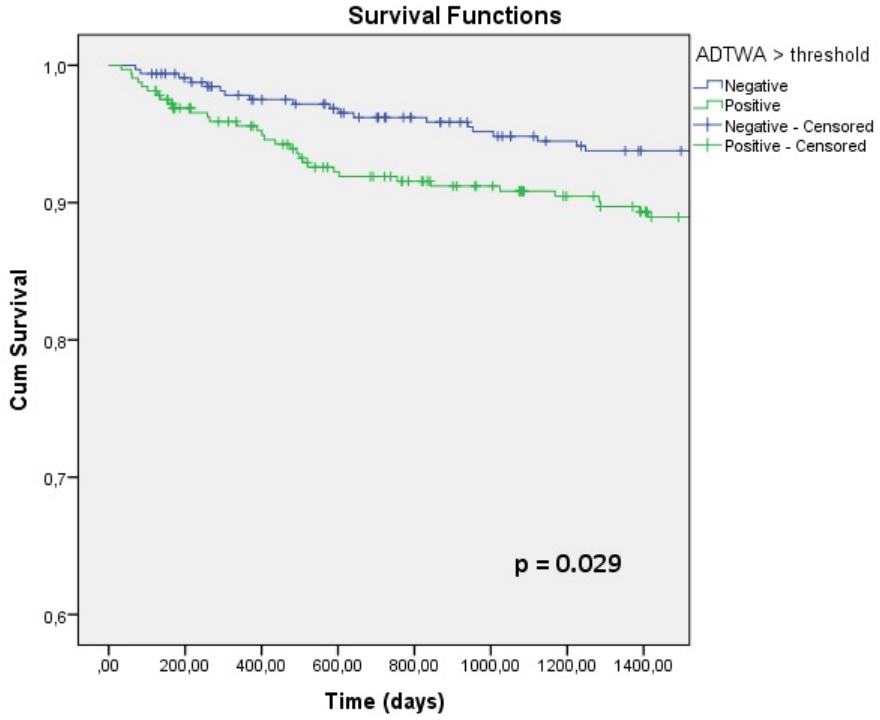

FIGURE 5.19: Kaplan Meier Survival Function for MM Method when alignment on T-wave is done (ADTWA threshold = $3.8024\mu V$)

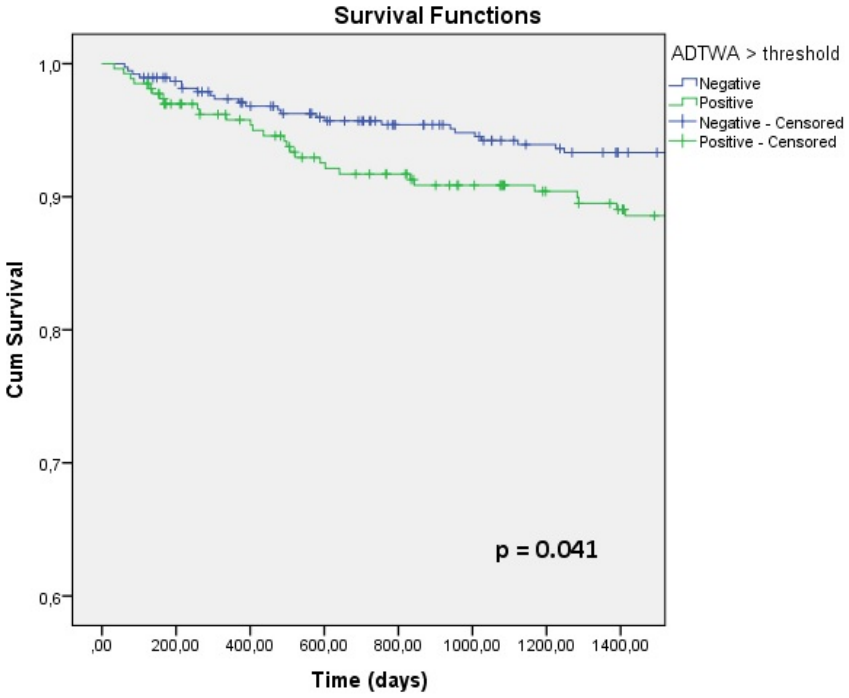

FIGURE 5.20: Kaplan Meier Survival Function for VM Method when alignment on T-wave is done (ADTWA threshold = $4.4751\mu V$)

5.2.3 ADTWA70 and ADTWA90

TWA values are naturally higher for faster heart rates, as evident from the boxplots represented before. So we checked analysis of TWA activity restricted only to certain bins of heart rate. The number of subjects for this analysis was lower as not every patient had a range of heart rates spanning from 60 bpm to 110 bpm. Results showed that only ADTWAI70 and ADTWAI90 were predictive for SCD whereas other bins of heart rate did not reach statistical significance. Results of the Log Rank test are reported in tables 5.7 and 5.8. Kaplan Meier survival curves are shown in fig. 5.21 and 5.22. Thresholds - derived from ROC Curves - and stastical p - values of Log Rank tests are reported.

	Threshold	Chi - square	df	Sig
AM Method	7.7516 μV	5.835	1	**0.016**
MM Method	3.5508 μV	5.319	1	**0.021**
VM Method	4.6746 μV	6.417	1	**0.011**

TABLE 5.7: Global comparisons - Log Rank (Mantel Cox) for ADTWAI70. In bold statistically significant results ($p < 0.05$).

	Threshold	Chi - square	df	Sig
AM Method	13.3859 μV	3.027	1	0.082
MM Method	9.8887 μV	7.613	1	0.06
VM Method	10.8411 μV	4.223	1	**0.04**

TABLE 5.8: Global comparisons - Log Rank (Mantel Cox) for ADTWAI90. In bold statistically significant results ($p < 0.05$).

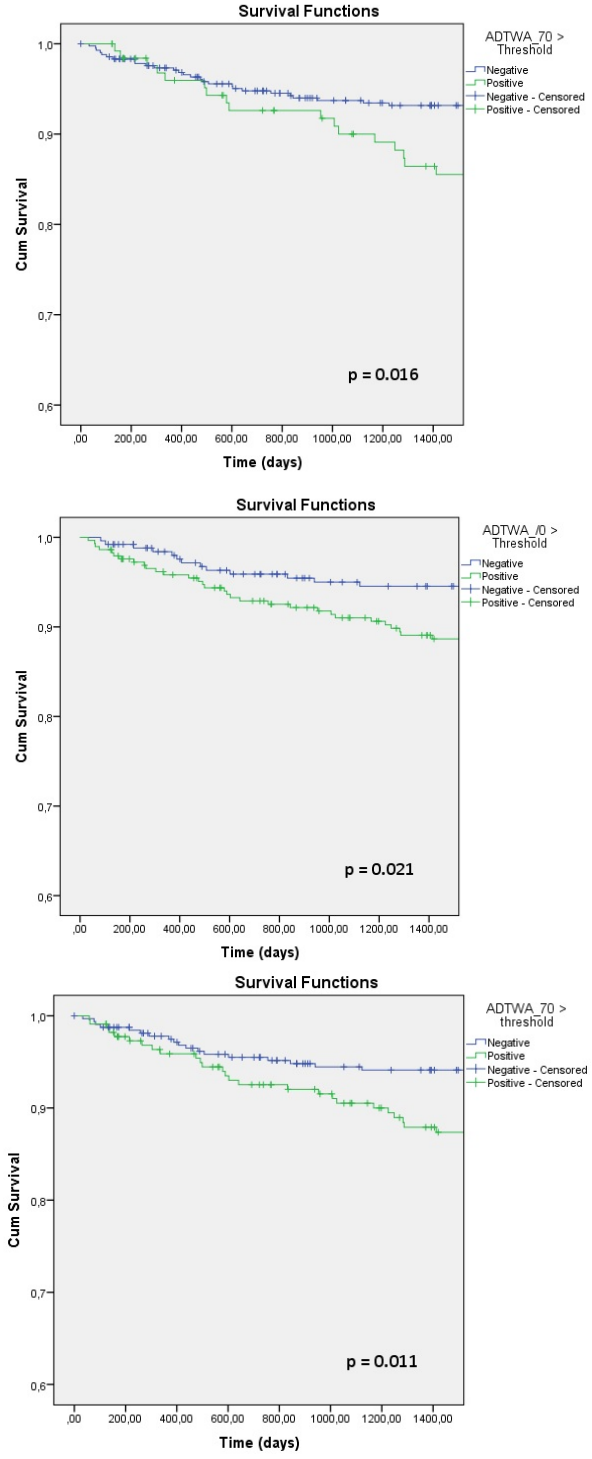

FIGURE 5.21: Kaplan Meier Survival Functions for ADTWAI70. From top to bottom : AM Method (ADTWA threshold = $7.7516\mu V$); MM Method (ADTWA threshold = $3.5508\mu V$); VM Method (ADTWA threshold = $4.6746\mu V$). T - wave alignment has been used in each of the three cases.

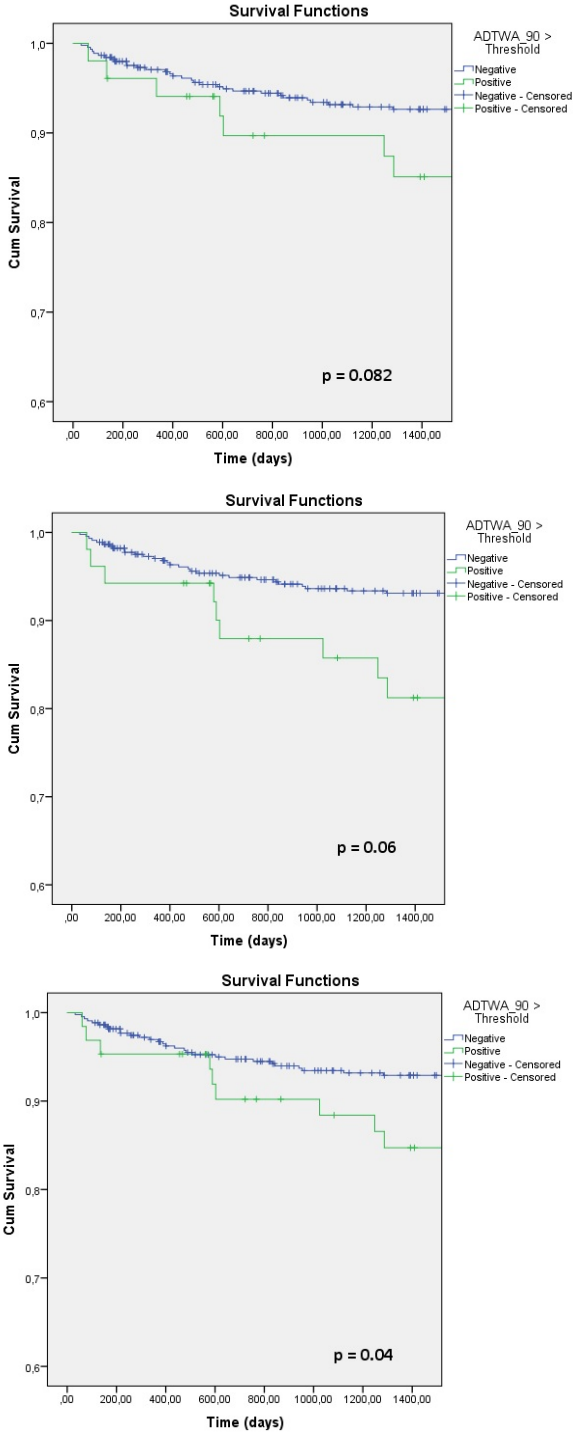

FIGURE 5.22: Kaplan Meier Survival Functions for ADTWAI90. From top to bottom : AM Method (ADTWA threshold = 13.3859μV); MM Method (ADTWA threshold = 9.8887μV); VM Method (ADTWA threshold = 10.8411μV). T - wave alignment has been used in each of the three cases.

Chapter 6

Discussion

The aim of the present work was to verify if a new index, simple, multi-lead and based on a physiological model, could be an efficient predictor for Sudden Cardiac Death.
TWA is an alteration in the T-wave morphology which has got the order of magnitude of microvolts, thus it can't be seen at a naked eye and some specific methods of signal processing are required. The first and most widely used are Spectral Method (SM)[14] and Modified Moving Average Method (MMAM)[27].
Both methods analyze TWA on a single-lead basis. In 2010 a new, multi-lead index was presented [25], based on periodic component analysis (πCA), a technique which tries to detect alternans enhancing its periodic characteristics. In 2012 [24] the index was applied to a database of 650 Holter electrocardiograms from patients with heart failure during sinus rhythm to evaluate whether the long-term average TWA activity on Holter monitoring provides prognostic information in patients with chronic heart failure. The average TWA activity measured automatically from Holter ECGs predicted SCD in patients with mild-to-moderate chronic heart failure.
In the meanwhile, another multilead method was developed (ADTWA) [15]. The index was based on a physiological model describing the genesis of T-wave [38]. After *methodological validation*[36] clinical validation, testing the index on predicting SCD was performed in the present study.
Every ECG was divided into segments in order to discharge those which were unsuitable for analysis. Then, predictive value was checked using three different methods. First attempt was to calculate the index on each segment kept for analysis and to do a global average on the 24 hours. Then a waveform for alternans was kept on each segment and eventually the maximum of the mean waveform - on the 24 hours - was taken as an index of TWA. The third index was obtained as the maximum of the module of the VCG (vectorcardiogram).
Prognostic value of the new index for SCD was confirmed, with a statistical significance similar to the one obtained in the previous work. Three indexes (ADTWA measured with AM Method, MM Method and VM Method) turned out to be good predictors of

SCD in patients with CHF. A restricted analysis only for ECG segments which had a mean heart rate comprised between 60 and 70 bpm turned out to be prognostic for SCD as well. This was not unexpected, as alternans is naturally higher at faster frequencies while high values for low heart rates may be indicators of anomalies in ventricular repolarization.
Thus ADTWA's methodological and clinical efficacy has been tested and these preliminary results suggest it can be used in clinical practice as a predictor of SCD.

Bibliography

[1] L. D. Metz A. K. Gehi R. H. Stein and J. A. Gomes. *Microvolt T-wave alternans for the risk stratification of ventricular tachyarrhythmic events: a meta-analysis.* J Am Coll Cardiol, 46(1):75–82, 2005.

[2] Antonis A. Armoundas, Gordon F. Tomaselli, and Hans D. Esperer. *Pathophysiological Basis and Clinical Application of T-Wave Alternans.* Journal of the American College of Cardiology Vol. 40, No. 2, 2002.

[3] Niebauer J Ashley EA. *Cardiology Explained.* Remedica, 2004.

[4] A. H. Huang B. D. Nearing and R. L. Verrier. *Dynamic tracking of cardiac vulnerability by complex demodulation of the T wave.* Science, no. 252, pp. 437–440, 1991.

[5] Lee KL Bardy GH and Mark DB et al. *Amiodarone or an implantable cardiovert-erdefibrillator for congestive heart failure.* N Engl J Med 2005;352:225237, 2006.

[6] Schumacher J. Benchimol A Desser KB. *Left anterior hemiblock from inferior infarction with left axis deviation. Chest.* Chest;61:74–76, 1972.

[7] Zipes DP Libby P Bonow RO Mann DL. *Braunwald's Heart Disease: A TextBook of Cardiovascular Medicine.* Saunders Elsevier, 2011.

[8] P P Dimitrow and J S Dubiel. *Echocardiographic risk factors predisposing to sudden cardiac death in hypertrophic cardiomyopathy.* Heart, 2005.

[9] Badilini F. et al. *Quantitative Aspects of Ventricular Repolarization: - Relationship Between Three Dimensional T Wave Loop Morphology and Scalar QT Dispersion.* A.N.E. Vol. 2, No. 2;146-157, 1997.

[10] Donoso E. Grishman A. *Spatial vectorcardiography II. Mod Concepts.* Cardiovasc Dis;30:693–696, 1961.

[11] Ruan Y. Guo X Jue X. *Model TJ-IV computer-assisted vectorcardiogram analysis system.* J Tongji Med Univ;21:22-81, 2001.

[12] Ma YX Wang ZC. et al. Guo XM Que XH. *Development and applications of an auto-analyzing system for model TJ-IV vector-cardiogram.* J Tongji Med Univ;21:22-81, 2005.

[13] Cambridge Heart. *Taking a MTWA Test.* URL: http://www.cambridgeheart.com/patients/taking-an-mtwa-test.

[14] C. R. Valeri J. N. Ruskin J. M. Smith E. A. Clancy and R. J. Cohen. *Electrical alternans and cardiac electrical instability.* Circulation, vol.77, no. 1, pp. 110–121, 1988.

[15] Mainardi LT and Sassi R. *Analysis of T Wave Alternans Using the Dominant T-wave paradigm.* Journal of Electrocardiology 44 (2), e6, 2011.

[16] Olmos S Martinez JP. *Methodological Principles of T Wave Alternans Analysis: A Unified Framework.* IEEE Transactions on Biomedical Engineering, Vol. 52, no. 4, 599, 2005.

[17] MedlinePlus. *Arrhytmias.* URL: http://www.nlm.nih.gov/medlineplus/ency/Book/001101.htm.

[18] MedlinePlus. *Heart pacemaker.* URL: http://www.nlm.nih.gov/medlineplus/ency/Book/007369.htm.

[19] MedlinePlus. *Holter Monitor (24h).* URL: http://www.nlm.nih.gov/medlineplus/ency/Book/003877.htm.

[20] MedlinePlus. *Implantable cardioverter-defibrillator.* URL: http://www.nlm.nih.gov/medlineplus/ency/Book/007370.htm.

[21] MedlinePlus. *Ventricular fibrillation.* URL: http://www.nlm.nih.gov/medlineplus/ency/Book/007200.htm.

[22] Walker ML and Rosenbaum DS. *Repolarization alternans: implications for the mechanism and prevention of sudden cardiac death.* Cardiovasc Res.;57:599–614, 2003.

[23] V. Monasterio and J. P. Martínez. *Multilead T-wave alternans quantification based on spatial filtering and the Laplacian likelihood ratio method.* DOI: 10.1109/CIC.2008.4749113 Conference: Computers in Cardiology, 2008.

[24] Violeta Monasterio et al. *Average T-wave alternans activity in ambulatory ECG records predicts sudden cardiac death in patients with chronic heart failure.* Heart Rhythm, Vol 9, No 3, March.

[25] Laguna P Martínez JP. Monasterio V Clifford GD. *A multilead scheme based on periodic component analysis for T-wave alternans analysis in the ECG.* Ann Biomed Eng.;38(8):2532-41., 2010.

[26] GB Moody. *T-Wave Alternans.* The PhysioNet / Computers in Cardiology Challenge, 2008.

[27] Verrier RL. Nearing BD. *Modified moving average analysis of T-wave alternans to predict ventricular fibrillation with high accuracy.* J Appl Physiol (1985).;92(2):541-9., 2002.

[28] Lehtimäki T Nieminen T and Viik J et al. *T-wave alternans predicts mortality in a population undergoing a clinically indicated exercise test.* Eur Heart J;28:2332–2337, 2007.

[29] Plonsey R Pilkington TC. *Engineering contributions to biophysical electrocardiography.* IEEE Press, New York, 1982.

[30] Rautaharju PM. *A hundred years of progress in electrocardiography. 2: The rise and decline of vectorcadiography.* Can J Cardiol;4:60–71, 1998.

[31] Filho CF Meneghini A Ferreira C Schapacknik E Dubner S Pérez Riera Uchida AH and Moffa P. *Significance of vectorcardiogram in the cardiological diagnosis of the 21st century.* Clin Cardiol.;30(7):319-23., 2007.

[32] Liew R. *Electrocardiogram-based predictors of sudden cardiac death in patients with coronary artery disease.* Clin Cardiol., 2011.

[33] K. Kumar R. L. Verrier and B. D. Nearing. *Basis for sudden cardiac death prediction by T-wave alternans from an integrative physiology perspective.* Heart Rhythm, 6(3):416 – 422, 2009.

[34] Antoni Bayes-Genis et al. Rafael Vazquez. *The MUSIC Risk score: a simple method for predicting mortality in ambulatory patients with chronic heart failure.* European Heart Journal, February 2009.

[35] Roberto Sassi and Luca Mainardi. *An Estimate of the Dispersion of Repolarization Times Based on a Biophysical Model of the ECG.* IEEE TRANSACTIONS ON BIOMEDICAL ENGINEERING, VOL. 58, NO. 1, 2011.

[36] Roberto Sassi and Luca Mainardi. *Theoretical comments on reproducibility and normalization of TWA measures.* J Electrocardiol.;46(2):132-5, 2013.

[37] Chou TC. *Value and limitations of vectorcardiography in cardiac diagnosis.* Cardiovasc Clin; 6:163–178, 1975.

[38] van Oosterom A. *Genesis of the T wave as based on an equivalent surface source model.* J Electrocardiol.;34 Suppl:217-27., 2001.

[39] Nearing BD Verrier RL and Kwaku KF. *Noninvasive sudden death risk stratification by ambulatory ECG-based T-wave alternans analysis: evidence and methodological guidelines.* Ann Noninvasive Electrocardiol;10:110 –120, 2005.

[40] Douglas P. Zipes and Hein J. J. Wellens. *Sudden Cardiac Death.* Circulation, 1998.